A comparison between advanced hybrid machine learning algorithms and empirical equations applied on abutment scour depth prediction

Khabat Khosravi*[1], Zohreh Sheikh Khozani[2], Luca Mao[3]

1- Department of Watershed Management Engineering, Ferdowsi University of Mashhad, Mashhad, Iran.
2- Institute of Structural Mechanics, Bauhaus Universität Weimar, 99423 Weimar, Germany.
3- School of Geography, University of Lincoln, Lincoln, UK.

*Corresponding author: K. Khosravi (Khabat.khosravi@gmail.com)

Abstract

Complex vortex flow patterns around bridge piers, especially during floods, cause scour process that can result in the failure of foundations. Abutment scour is a complex three-dimensional phenomenon that is difficult to predict especially with traditional formulas obtained using empirical approaches such as regressions. This paper presents a test of a standalone Kstar model with five novel hybrid algorithm of bagging (BA-Kstar), dagging (DA-Kstar), random committee (RC-Kstar), random subspace (RS-Kstar), and weighted instance handler wrapper (WIHW-Kstar) to predict scour depth (*ds*) for clear water condition. The dataset consists of 99 scour depth data from flume experiments (Dey and Barbhuiya, 2005) using abutment shapes such as vertical, semicircular and 45° wing. Four dimensionless parameter of relative flow depth (h/l), excess abutment Froude number (Fe), relative sediment size (d_{50}/l) and relative submergence (d_{50}/h) were considered for the prediction of relative scour depth (ds/l). A portion of the dataset was used for the calibration (70%), and the remaining used for model validation. Pearson correlation coefficients helped deciding relevance of the input parameters combination and finally four different combinations of input parameters were used. The performance of the models was assessed visually and with quantitative metrics. Overall, the best input combination for vertical abutment shape is the combination of F_e, d_{50}/l and h/l, while for semicircular and 45°

wing the combination of the Fe and d_{50}/l is the most effective input parameter combination. Our results show that incorporating Fe, d_{50}/l and h/l lead to higher performance while involving d_{50}/h reduced the models prediction power for vertical abutment shape and for semicircular and 45° wing involving h/l and d_{50}/h lead to more error. The WIHW-Kstar provided the highest performance in scour depth prediction around vertical abutment shape while RC-Kstar model outperform of other models for scour depth prediction around semicircular and 45° wing.

Keywords: Abutment, scour depth, machine learning, empirical models.

1. Introduction

Bridges are critical infrastructures, and the failure of their piers can lead to severe economical and social consequences. The most common failure mode for bridges over rivers is generally due to intense local scouring around their piers. Therefore, a reliable estimation of abutment scour and its disruptive effects are crucially important to design these infrastructures as overestimating or underestimating scour can result in higher construction cost and abutment failure, respectively (Azamathulla et al., 2009; Cardoso and Bettess, 1999). Bridge abutments change the local flow pattern and generally cause the formation of a three-part separation zone around a bridge pier. The pressure gradient due to the presence of the pier forces a down-flow that causes the scouring in front of the pier. This leads to the generation of a so-called horseshoe vortex which facilitate further the scouring in front of pier (Melville and Coleman, 2000; Török et al., 2014). The shear stresses at the upstream face of an abutment due to the principal vortices also facilitate secondary vortices. In addition, unsteady shear layers that are generated at the pier rotate in vertical axes (wake vortices) as small eddies. Furthermore, bow-waves can also contribute to the scouring process. A combination of these vortexes eventually lead to scour holes around piers of bridges

(Laursen and Toch, 1956; Liu et al. 1961; Kwan, 1988; Hosseini et al., 2016), and detailed descriptions on abutment scour depth process are widely available in the literature (e.g., Dey, 1997; Dey and Barbhuiya, 2005; Gazi et al., 2019; Kothyari et al., 1992; Melville and Raudkivi, 1977; Melville and Sutherland, 1988; Moonen and Allegrini, 2015; Namaee and Sui, 2019; Raudkivi and Ettema, 1983).

A local scour can be created in conditions in which no sediments are proceeding from upstream reaches (i.e., clear water, or no sediment feeding from upstream) or in more natural conditions in which the flow approach the pier with sediments (i.e., sediment is fed from upstream reaches). A wide range of experimental and field studies investigated the process of scour depth around bridges under clear water conditions, due to the simplicity of this condition. Dey and Lambert (2005) conducted experiments under clear water conditions and investigated the evolution over time and the equilibrium conditions of scour depth for three different shapes of short abutments (vertical wall, semicircular, and 45° wing wall) using both uniform and nonuniform sediments. They applied the concept of mass conservation of sediment to derive numerical equations to calculate the scour depth evolution over time. Oliveto and Hager (2002) conducted a further set of experiments and proposed an equation that allows to calculate the scour depth around both piers and abutments that worked reasonably well when applied to other experimental datasets too, especially for rectangular cross section and uniform distribution of roughness. Amini et al. (2012) further revealed that the pile spacing, diameter, and the submerge ratio are three important parameter which can affect the scour depth. Although many flume experiments have been carried out to support scour depth modeling (Ataie-Ashtiani et al., 2010; Ataie-Ashtiani and Beheshti, 2006; Singh et al., 2020; Yang et al., 2020), this approach suffers from scale effect issues which can have an impact on the applicability of the results. Also, the experimental approach is costly and time-consuming. Flume experimental data are generally used to derive empirical equations based on regressions but this approach, albeit practical, are too simplistic to represent the complexity of flows around a bridge piers (Azamathulla et al., 2009). Numerical investigations of scour depth have been attempted using SSIIM models (Hamidi and Siadatmousavi, 2018; Jahangirzadeh et al., 2014), Smagorinsky subgrid model combined with a ghost-cell immersed boundary method (Kim et al., 2014), Virtual Flow Simulator (VFS-Geophysics) (Khosronejad et al., 2020), FLUENT (Yang et al., 2005), and FLOW-3D (Omara et al., 2019), but applications of these models are restricted due to the paucity of large experimentally and field measurement dataset for their calibration and validation. Although these models consider the physics of the scouring processes, their implementation is difficult, time consuming, and needs large and accurate datasets.

An alternative to traditional approaches is provided by the use of Artificial Intelligence (AI) as it is user-friendly, easy to perform, requires less data, is robust to missing data, and provides high accuracy to predict complex phenomena especially in engineering and geoscience fields. Artificial intelligence has the ability to train complex and hidden relationships between inputs and outputs without a detailed knowledge of the physics of the problem. Employing AI for predicting scour depth around different hydraulic structures has indeed been attempted in literature in the past decade (Ebtehaj et al., 2018; Guven and Azamathulla, 2012; Guven and Gunal, 2008; Najafzadeh et al., 2013a; Najafzadeh and Lim, 2015).

Artificial Neural Networks (ANN) is the traditional and most widely used algorithm for scour depth prediction (Amini et al., 2012; Kaya, 2010; Yazdandoost and Birgani, 2011). Three different ANN techniques as the Feed Forward Back Propagation (FFBP), Feed Forward Cascade Correlation (FFCC) and Radial Basis Function (RBF) were applied by Muzzammil

(2008) to estimate scour depth in clear-water condition for vertical wall abutments. In his study the input and output data were normalized (0 and 1) and the impact of dimensionless and dimensional inputs in modeling the scour depth was investigated. There were only a few later application of ANN models due to many critical disadvantages as the low speed convergence and poor generalization power (Choubin et al., 2018; Hooshyaripor et al., 2014). Also, the performances of the ANN model strongly depend of the extension of the dataset (Hooshyaripor and Tahershamsi, 2013). To overcome this issue, adaptive Neuro-Fuzzy Inference System (ANFIS) was developed as an ensemble of ANN and fuzzy logic. Bateni and Jeng (2007) employed an ANFIS method to simulate the scour depth. Hosseini et al. (2016) compared the prediction power of ANFIS, ANN and multiple nonlinear regression (MNLR) for scour depth perdition and finally stated that the ANFIS model has a higher prediction capability than ANN and MNLR models. Still, the ANFIS model suffers from determining the weights in a membership function, which affect significantly the result. Abd El-Hady Rady (2020) reported on the superiority of genetic programming (GP) over ANFIS algorithm for scour depth around bridge pier. Support Vector Machine (SVM) is another type of neuron-based model which was successfully applied in scour depth prediction. Parsaie et al. (2019) observed that the SVM model has a higher prediction capability for scour depth prediction than ANN and ANFIS algorithm. Ahmad et al., (2018) revealed that SVM is sensitive to hyper-parameter selection, and Najafzadeh et al. (2016) reported that ANFIS performed better than SVM and traditional existing equations. Further, the Group Method of Data Handling (GMDH) is a model which can automatically select the number of neurons and the network layers and allows to obtain a mathematical model in terms of polynomials for the target parameter. However, being a kind of neuron-based model, GMDH is sensitive to the extension of the dataset. Najafzadeh et al. (2013)

applied both GMDH and SVM approaches to a set of experimental data to predict scouring depth in four different shapes of abutments in both clear water and sediment feeding conditions. They used a backward path (BP) algorithm to design topology of the GMDH model in order to improve the performance of model and discovered that the BP-GMDH performed better than the SVM in both conditions. Scour depth around abutments was also predicted by using the pareto evolutionary structure of ANFIS network by Azimi et al. (2017; 2019). Using the dataset from Dey and Lambert (2005) they used a sensitivity analysis to rank the role of eleven different dimensional input variables which effect scour depth. Also, they compared their best developed model (i.e., ANFIS-GA/SVD 7) with other techniques employed previously (i.e., Azamathulla, 2012; Moradi et al., 2019; Muzzammil, 2010; Najafzadeh et al., 2013b) and revealed that the ANFIS-GA/SVD model could provide more accurate results of scour depth in comparison with GEP, ANFIS–SC, ANFIS and GMDH models. Extreme Learning Machine (ELM) is another neuron-based algorithm with faster training phase and has been successfully applied in a different field of study. Ebtehaj et al. (2018) reported that the ELM model has a higher performance than ANN and SVM models to predict scour depth. In a recent study, Bonakdari et al. (2020) used the ELM technique to predict scour depth in clear-water condition considering four different nondimensional input parameters to estimate scour depth. About 11 different input combinations were tested to find the best one and they finally concluded that the model which contains all input variables allowed to obtain a better performance. They extended a matrix-based equation to calculate the scour depth, but their equation is highly complex and need large mathematic calculations. Because ELM is a version of the ANN model, its performance strongly depends on the extent of the dataset and is hampered by low performances with small datasets.

To overcome the shortcomings of the aforementioned traditional machine learning algorithm, different kind of data mining algorithms have been recently developed. These are tree-based [random forest (RF), random tree (RT), M5 prime (M5P), reduced error pruning tree (REPT)], rule-based [M5 Rule (M5R)], lazy-learn-base [Kstar, instance-based K-nearest neighbors (IBK), locally-weighted learning (LWL)], regression-based [sequential minimal optimization regression algorithm (SMO)] and ensemble-based [bagging (BA), random committee (RC), random subspace (RS)] algorithms. Some of these techniques operate for classification as well as for regression, based on the learner. The superiority of the RF algorithm over ANN and SVM in infiltration process prediction was reported by Sihag et al. (2020). Also, Yan et al. (2012) found that M5P algorithm had a higher prediction capability than ANN model for daily suspended sediment load prediction. Different metaheuristic algorithms were applied to solve the weakness of neuron-based models which suffer from determination of weights in membership function and operators. Khosravi et al. (2019a) compared predictive modeling of standalone new algorithms of M5P, RT, RF, REPT, Kstar with standalone and optimized ANFIS model using metaheuristic algorithms for reference evaporation prediction. They found that new a decision-tree based standalone model and Kstar models have higher performance than the ANFSI model, while optimized ANFIS models performed slightly better than standalone new models. Except for better prediction power and more flexibility, new algorithms require fewer parametric settings, making them more practical for real applications.

Sheikh Khozani et al. (2019) employed different standalone and a hybrid model to predict apparent shear stress in compound channels. They found that the BA-M5P model predicted the apparent shear stress with higher accuracy than standalone models. Khosravi et al. (2020) implemented four standalone algorithm of decision tree and four ensemble-based model using

BA algorithm for bedload transport rate prediction, and found that ensemble-based models predicted bedload with higher prediction accuracy. Similar observations have been reported by Bui et al. (2020b) and Khosravi et al. (2018).

The main objective of the present study is to predict abutment scour depth using a suite of new standalone and ensemble-based models. To meet the aim, standalone KStar algorithm are applied as a base model along with five novel ensemble-based models of BA-KStar, dagging (DA-KStar), RC-Kstar, RS-Kstar and Weighted Instance Handler Wrapper model (WIHW-Kstar). Finally, the results are compared with two traditional empirical equations (Dey and Barbhuiya, 2005 and Muzzammil, 2010) as a benchmark.

2. Methodology

2.1. Identifying effective parameters

Scour depth (d_s) at abutment or around bridge piers depends on the sediment feeding conditions from upstream. Indeed, experiments can be designed with a certain rate of sediment supply from upstream (as generally expected in the field during flood events) or without coarse sediment supply (i.e., clear water conditions). Overall, the scour depth abutment has been considered as a function of sediment size, flow parameters, and the geometrical characteristics of the structure (Bonakdari et al., 2020; Firat and Gungor, 2009; Raudkivi and Ettema, 1983; Sheppard et al., 2004). This can be written as follows:

$$d_s = f(U, U_c, l, b, g, K_s, d_{50}, h, \rho, \rho_s, \upsilon) \quad (1)$$

Where U = average flow velocity; U_c = critical sediment velocity; l = transverse abutment length; b = stream wise length; g = acceleration due to gravity; K_s = abutment form factor; d_{50} = median sediment diameter; h = approach flow depth; ρ = fluid density; ρ_s = sediment density;

and υ = fluid kinematic viscosity. As K_s is the same for each cross section, and ρ, ρ_s are constant, these three parameters can be removed from the list. According to several approaches in literature, and considering that dimensionless parameters are generally to be preferred, it can be said that:

$$\frac{d_s}{l} = f(F_e, \frac{d_{50}}{l}, \frac{d_{50}}{h}, \frac{h}{l}) \tag{2}$$

where F_e is defined as an excess abutment Froude number:

$$F_e = U / \sqrt{gl(S-1)} \tag{3}$$

where S is the specific gravity of sediment defined as the ratio of sediment density to fluid density. Because *b/l* was constant for the dataset used in this paper (see next chapter) it was removed from the list of effective input parameters.

2.2. Dataset collection and preparation

In this study we used the Dey and Barbhuiya (2005) dataset referring to relative scour depth around bridge abutment (*ds/l*) for clear water conditions using uniform bed sediments. The dataset of Dey and Barbhuiya (2005) consists of 295 runs carried out in the hydraulic laboratory of the technology institute in India for three abutment shape (i.e. each set is about 99 data). Their experiments were performed on a 20 m long, 0.9 m wide, and 0.7 m deep flume. They used three type of abutment shape, vertical wall, 45° wing wall, and semicircular which were made from Plexiglas in five different sizes (Fig 1 and Table 1 and 2).

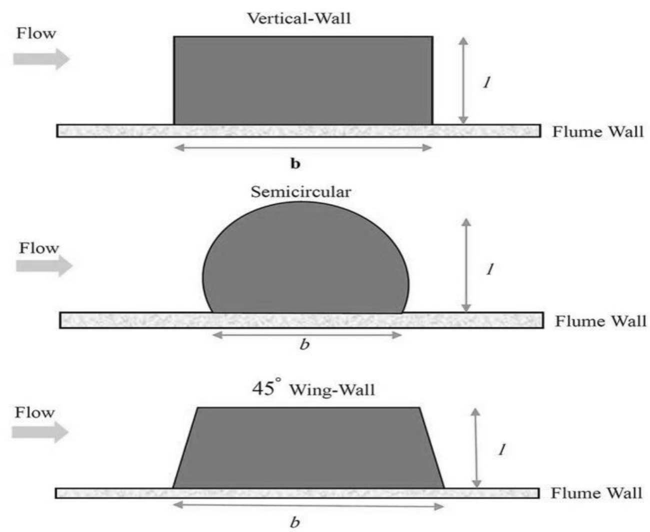

Fig 1. Schematic diagram of scouring at an abutment: (a) vertical wall, (b) semicircular and (c) 45° wing wall. [*b* is the streamwise length and *l* is the transverse length of abutments]

Each abutment was placed in a bed sediment recess of 2.4 m long, 0.9 m wide, and 0.3 m deep appended to the flume wall. A V-notch weir embedded at the inlet of the flume was used for measuring discharge. A mechanical point gauge was used for flow adjusting and finally measured through Vernier point gauge with a veracity of ±0.1 mm. All experiments were carried out without feeding sediments (i.e., clear water) with $U/U_c < 0.95$ for a period of 48-50 h, until equilibrium conditions (i.e., no further morphological changes) were reached. All experiments were performed in a condition of short abutment physical model (i.e., $h/l > 1$). Barbhuiya (2003) and Dey and Barbhuiya (2005) provide further details on the experimental runs and conditions. In the present work, after compiling the dataset, the data was spilt into two main groups randomly, with 70% of data (69 dataset) being used for developing the model, while the remaining 30% (30 dataset) was used for validating purpose.

Table 1. Main characteristics of the dimensionless data for the training (a) and the testing (b) dataset from Dey and Barbhuiya (2005)

(a)	Vertical					Semi-circular					45 degree				
Parameters	Max	Min	Mean	STD	Skew	Max	Min	Mean	STD	Skew	Max	Min	Mean	STD	Skew
d_{50}/l	0.05	0.00	0.01	0.01	0.05	0.08	0.00	0.01	0.01	2.32	0.08	0.00	0.01	0.01	2.32
h/l	6.25	0.48	2.37	1.42	6.25	6.25	0.38	2.41	1.44	1.02	6.25	0.59	2.45	1.39	1.02
d_{50}/h	0.02	0.00	0.01	0.01	0.02	0.02	0.00	0.01	0.01	1.04	0.02	0.00	0.01	0.01	1.14
Fe	0.68	0.16	0.33	0.13	0.68	0.83	0.17	0.33	0.14	1.42	0.83	0.17	0.33	0.13	1.51
ds/l	3.70	0.98	2.07	0.64	3.70	3.38	0.71	1.67	0.62	0.73	3.78	0.76	1.76	0.63	1.02

(b)	Vertical					Semi-circular					45 degree				
Parameters	Max	Min	Mean	STD	Skew	Max	Min	Mean	STD	Skew	Max	Min	Mean	STD	Skew
d_{50}/l	0.08	0.00	0.01	0.02	2.84	0.05	0.00	0.01	0.01	1.52	0.05	0.00	0.01	0.01	1.37
h/l	6.25	0.58	2.42	1.39	1.06	6.25	0.45	2.29	1.41	1.07	6.25	0.61	2.43	1.38	1.12
d_{50}/h	0.02	0.00	0.01	0.00	1.44	0.02	0.00	0.01	0.01	1.28	0.02	0.00	0.01	0.00	1.16
Fe	0.83	0.17	0.32	0.14	1.90	0.65	0.15	0.31	0.13	1.17	0.65	0.19	0.33	0.12	1.01
ds/l	4.35	1.13	2.08	0.71	1.37	3.10	0.65	1.58	0.60	0.86	3.15	1.00	1.75	0.62	0.77

Table 2. Main characteristics of the dataset for the training (a) and the testing (b) dataset from Dey and Barbhuiya (2005)

(a)	Vertical					Semi-circular					45 degree				
Parameters	Max	Min	Mean	STD	Skew	Max	Min	Mean	STD	Skew	Max	Min	Mean	STD	Skew
d_{50} (m)	0.003	0.000	0.001	0.001	1.285	0.003	0.000	0.001	0.001	1.239	0.003	0.000	0.001	0.001	1.322
h (m)	0.250	0.058	0.161	0.065	-0.169	0.250	0.050	0.164	0.064	-0.330	0.250	0.059	0.163	0.065	-0.190
ds (m)	0.293	0.068	0.156	0.055	0.715	0.258	0.055	0.123	0.056	1.022	0.274	0.053	0.125	0.052	0.983
l (m)	0.120	0.040	0.080	0.028	0.000	0.130	0.040	0.080	0.032	0.201	0.100	0.040	0.075	0.024	-0.361
b (m)	0.240	0.080	0.160	0.057	0.000	0.260	0.080	0.080	0.063	0.201	0.300	0.120	0.075	0.071	-0.361

(b)	Vertical					Semi-circular					45 degree				
Parameters	Max	Min	Mean	STD	Skew	Max	Min	Mean	STD	Skew	Max	Min	Mean	STD	Skew
d_{50} (m)	0.003	0.000	0.001	0.001	1.572	0.002	0.000	0.001	0.001	1.109	0.003	0.000	0.001	0.001	1.347
h (m)	0.250	0.058	0.166	0.063	-0.257	0.250	0.050	0.158	0.069	-0.076	0.250	0.059	0.163	0.063	-0.324
ds (m)	0.287	0.078	0.153	0.051	0.840	0.240	0.058	0.112	0.045	1.172	0.269	0.061	0.127	0.053	1.174
l (m)	0.120	0.040	0.079	0.029	-0.008	0.130	0.040	0.078	0.034	0.633	0.100	0.040	0.075	0.023	-0.352
b (m)	0.240	0.080	0.159	0.059	-0.008	0.260	0.080	0.078	0.068	0.633	0.300	0.120	0.075	0.070	-0.352

2.3. Input combination

Because some input parameters are more important or relevant than others, it is important to exclude those that hamper the modeling performance without improving the effectiveness of the modeling. To select the best input array, four different input combinations were constructed based on the Pearson correlation coefficient and finally tested in order to find the most effective one. To start with, the parameter with the highest degree of Pearson correlation coefficient (r)

was considered as the first input parameter to the model. The assumption is that the parameter with the highest correlation with the output has a better ability to predict the output with higher accuracy. Then, the next parameter with the next highest r value was added to the first input and the selection "input No.2" was defined. This process continued until the parameter with the lowest r value was added to the combination of input parameters and the selection "input No.4" was defined (Table 3). The most effective input combination was identified by comparing the effectiveness of each input combination using the root mean square error (RMSE).

Table 3. Selection of the different input parameters.

Input No.	Input parameters	Outputs	Input parameters	Outputs
1	F_e	$ds/l_{(V,\,S)}$	F_e	$ds/l_{(45°)}$
2	F_e, d_{50}/l	$ds/l_{(V,\,S)}$	F_e, d_{50}/l	$ds/l_{(45°)}$
3	F_e, d_{50}/l, h/l	$ds/l_{(V,\,S)}$	F_e, d_{50}/l, d_{50}/h	$ds/l_{(45°)}$
4	F_e, d_{50}/l, h/l, d_{50}/h	$ds/l_{(V,\,S)}$	F_e, d_{50}/l, d_{50}/h, h/l	$ds/l_{(45°)}$

V, S and 45° are Vertical − Wall, Semicircular and 45°Wing − Wall

2.4. Sensitivity analysis

A sensitivity analysis was performed in order to determine the effectiveness of each input parameter. To do that, at first all parameters were combined and considered as an input to the model (i.e. No. Total). Next, four different combinations of parameters were considered (i.e. No. A, B, C, and D) and in each combined parameter one of the input parameters was removed (Table 4). Similar to the previous section, RMSE was used as criterion to determine the range of changes, as removing the most effective parameter would lead to the highest degree of error.

Table 4. Parameters considered in the sensitivity analysis

No.	Input parameters	Removed parameter

A	Fe, d_{50}/l, h/l	d_{50}/h
B	Fe, d_{50}/l, d_{50}/h	h/l
C	Fe, h/l, d_{50}/h	d_{50}/l
D	d_{50}/l, h/l, d_{50}/h	Fe
Total	Fe, d_{50}/l, h/l, d_{50}/h	---

2.5. Models parameter optimization

Apart from the quality of the dataset, a proper selection of input parameters and the modeling prediction capability determine the optimum values for each model operators and have a significant effect on the predictive power of the model. In the present study, a trial-and-error approach was applied to determine the optimum value for each operator. The models were first run using a range of default values, and then the values were adjusted arbitrary until converging to optimal values which led to the lowest RMSE.

2.6. Model theory background

2.6.1. Kstar

This is an instance-base model that classifies an instance by contrasting it to a pre-classified sample dataset. Similar examples lead to similar classifications and this is the main assumption of the Kstar model. The associated elements of an instance-based trainee are the distance function that defines how similar two examples are, and the classification function that determines how similar examples give the new example an ultimate classification (Cleary and Trigg, 1995). The K-star method employs entropic measurements related to the probability of turning a sample into another by selecting randomly between all feasible transformations. The transformation of an example into another one is attained by mapping one instance to another by determining a finite set of transformation, and then one instance (m) is converted into a finite sequence of transformations (n) beginning at (a) and ending at (b). Assuming the defined transformation S and a value of this set s, maps $I \rightarrow I$. For mapping instance with itself β is employed in $S(\beta(a) = a)$. The parameter β terminates the set of all codes of S^* as P.

$$\bar{s}_a = s_n\big(s_{n-1}(\dots s_1(a) \dots)\big) \quad s = s_1 \dots . s_n \tag{4}$$

The probability function of S^* is P which satisfies properties as:

$$0 \leq \frac{p(\bar{s}u)}{p(\bar{s})} \leq 1 \tag{5}$$

$$\sum_u p(\bar{s}u) = p(\bar{s}) \tag{6}$$

$$p(\Lambda) = 1 \tag{7}$$

$$\sum_{s \in p} p(\bar{s}) = 1 \tag{8}$$

The probability function P^* is defined as:

$$P^*\left(\frac{b}{a}\right) = \sum_{s \in p: s(a) = b} P(s) \tag{9}$$

Finally, the Kstar function defined as:

$$k^*\left(\frac{b}{a}\right) = -log_2 P^*\left(\frac{b}{a}\right) \tag{10}$$

2.6.2. Bagging model

Machine learning implementations suggest that any given learning model can outperform all others for a specific issue or for a specific subset of input data, but it is rare to find a single expert that achieves good outcomes on an entire given problem (Dietterich, 2000). Bagging is one of the most well-known ensembles learning algorithms (Oza, 2005), and is also known as bootstrap aggregation (Breiman, 1996). The bagging model can improve the classification precision in machine learning (ML) and by decreasing the variance can leadsto prevent overfitting. This model is commonly applied to decision tree-based algorithms (Dietterich, 2000). The bagging model procedure follows three steps: a) bootstrap samples are collected by resampling as arbitrarily of the training dataset to develop a set of training subsets; b) several classifier-based models are designed using each of the sub-sets; and finally, c) the terminal method comprises of the aggregation of all classifier-based models.

2.6.3. Dagging model

The Dagging algorithm presented by Ting and Witten (1997) is an ensemble of algorithms. Like the bagging, the approach focuses at achieving a reliable model of classification by integrating the poor learners trained on various samples of the training set. However, the Dagging model utilizes disjointed, stratified samples instead of bootstrapping, and it is a powerful method when the individual classifiers have a bad time complexity.

2.6.4. Random Subspace model

The Random Subspace method (RSS; Ho, 1998) is another ensemble learning technique that combines several classifiers trained on randomly chosen subspace features. This algorithm is randomly selected by the original training set to make the training subset (Kotsiantis, 2011). Therefore, the series features a subset of each sub-classifier training at the final prediction outcomes achieved by a combination of voting methods (Sun and Zhang, 2007). When considering the situation with n observations in a k dimensional space, then:

$$\left\{\left(\left(x_{1j}, x_{2j}, \ldots, x_{ij}, \ldots, x_{kj}\right)\middle| x_{ij}\right)\right\}, \quad where\ i \in \{1, n\}, j \in \{1, k\} \tag{11}$$

where i and j are the number of observation and variables, respectively. The RSS developed by selecting the variables randomly is shown as follows:

$$\left\{\left(\left(x_{1j}, x_{2j}, \ldots, x_{ij}, \ldots, x_{kj}\right)\middle| x_{ij}\right)\right\}, as \quad \begin{cases} x_{ij} = x_{ij} & for\ i \in I \\ x_{ij} = Null & for\ i \notin I \end{cases} \tag{12}$$

in which I is k' dimensional subsect and $k' \leq k$. Every time, a random producer from 1 to k' is employed to choose a variable to be applied in the subspace, and the procedure is repeated k' times. As an outcome, N random subspaces are generated as various filters for the identified issue. On top of those filters, a similar algorithm is applied to produce various decision agents. This method represents a type of stochastic discrimination to improve prediction performance by combining poor models with no maximum discriminating power for the same issue (Ho, 1998).

2.6.5. Random Committee model

The Random Committee (RC) approach produces a set of main classifiers (random trees) and creates their estimation by combining predictions of probability. Every main classifier is based on similar data but employs another gene random number. It only becomes meaningful when randomizing the main classifier, otherwise all classifiers will be equivalent.

2.6.6. Weighted Instance Handler Wrapper model

In this algorithm, a general wrapper technique around any classifier allows for weighted instances support. This approach benefit from a weight resampling if the interface is not enforced by the base classifier and instances weights other than 1.0. The learning data is transferred to the base classifier by default when it can manage instance weights. Anyway, implementing resampling technique with weights is applicable as well.

2.6.7. Dey and Barbhuiya equation

In their original paper, Dey and Barbhuiya (2005) proposed empirically derived equations for each shape of abutments as such:

$$\frac{d_s}{l} = 7.281(F_e)^{0.314}\left(\frac{h}{l}\right)^{0.128}\left(\frac{l}{d_{50}}\right)^{-0.167} \qquad for\ Vertical\ wall\ abutments \tag{13}$$

$$\frac{d_s}{l} = 8.319(F_e)^{0.312}\left(\frac{h}{l}\right)^{0.101}\left(\frac{l}{d_{50}}\right)^{-0.213} \qquad for\ 45^{\circ}\ wall\ abutments \tag{14}$$

$$\frac{d_s}{l} = 8.689(F_e)^{0.192}\left(\frac{h}{l}\right)^{0.103}\left(\frac{l}{d_{50}}\right)^{-0.296} \qquad for\ Semicircular\ abutments \tag{15}$$

where d_{50} is the median diameter of sediment particles, d_s is the equilibrium scour depth, h is the approaching flow depth, l is the transverse length of abutment, and F_e is the excess abutment Froude number

2.6.8. Muzzammil equation

The performance of three ANFIS, ANN and conventional regression-based models for estimating scour depth in clear-water condition was investigated by Muzzammil (2010). He obtained a conventional regression model which depended on four different nondimensional parameters to calculate the scour depth at the abutments as:

$$\frac{d_s}{l} = 9.694K_s(F_e)^{0.648}\left(\frac{h}{l}\right)^{0.04}\left(\frac{d_{50}}{l}\right)^{-0.075} \tag{16}$$

Equation (16) was proposed for all three different geometry of abutments (vertical-wall, 45° wing-wall, and semicircular).

2.7. Model evaluation

All approaches are finally compared in terms of their power of prediction. Here a portion (30%) of the original dataset was used for validation purposes, and we used both graphical methods (line graphs, scatter plots and violin plots) and quantitative metrics to evaluate the performance of each approach. A ranking of performance was achieved using quantitative metrics including RMSE, relative RMSE (RRMSE), Nash-Sutcliffe efficiency index (NSE), Willmott's index of agreement (WI), and Legates and McCabe coefficient of efficiency (LM) that were computed as follows:

$$RMSE = \sqrt{\frac{1}{N}\sum_{i=1}^{N}(d_s^{Obs} - d_s^{\mathrm{Pre}})^2}, \qquad 0 \le RMSE \le +\infty \qquad (17)$$

$$RRMSE = \frac{\sqrt{\frac{1}{N}\sum_{i=1}^{N}(d_s^{Obs} - d_s^{\mathrm{Pre}})^2}}{\sum_{i=1}^{N} d_s^{Obs}}, \qquad 0 \le RRMSE \le +\infty \qquad (18)$$

$$NSE = 1 - \left[\frac{\sum_{i=1}^{N}(d_s^{Obs} - d_s^{\mathrm{Pre}})^2}{\sum_{i=1}^{N}(d_s^{Obs} - \bar{d}_s^{Obs})^2}\right], \qquad -\infty < NSE \le 1 \qquad (19)$$

$$WI = 1 - \left[\frac{\sum_{i=1}^{N}(d_s^{Obs} - d_s^{\mathrm{Pre}})^2}{\sum_{i=1}^{N}(\left|d_s^{\mathrm{Pre}} - \bar{d}_s^{Obs}\right| + \left|d_s^{Obs} - \bar{d}_s^{Obs}\right|)^2}\right], \qquad 0 \le \mathrm{WI}_{\mathrm{E}} \le 1 \qquad (20)$$

$$LM = 1 - \left[\frac{\sum_{i=1}^{N}\left|d_s^{\mathrm{Pre}} - d_s^{Obs}\right|}{\sum_{i=1}^{N}\left|d_s^{Obs} - \bar{d}_s^{Obs}\right|}\right], \qquad 0 \le LM_E \le 1 \qquad (21)$$

where N is the number of data sample, while d_s^{Pre}, d_s^{Obs}, and d_s^{Obs}, are the predicted, observed and mean of the observed scour depth, respectively.

3. Results and discussion

3.1. The importance of the input variables

Each input parameter has a different relative effectiveness on the result. The relative importance of these parameters for each abutment shape was assessed through the Pearson correlation coefficient (r) and is shown in Fig 2. Results reveal that the F_e parameter has the highest effect on the scour depth prediction at each shape of Vertical – wall (r =0.978), Semicircular (r =0.964) and 45° wing – wall (r =0.957), followed by d_{50}/l (r =0.920, 0.906 and 0.910 respectively), h/l (r =0.614, 0.518 and 0.528 respectively) and d_{50}/h (r =0.439, 0.508 and 0.512 respectively).

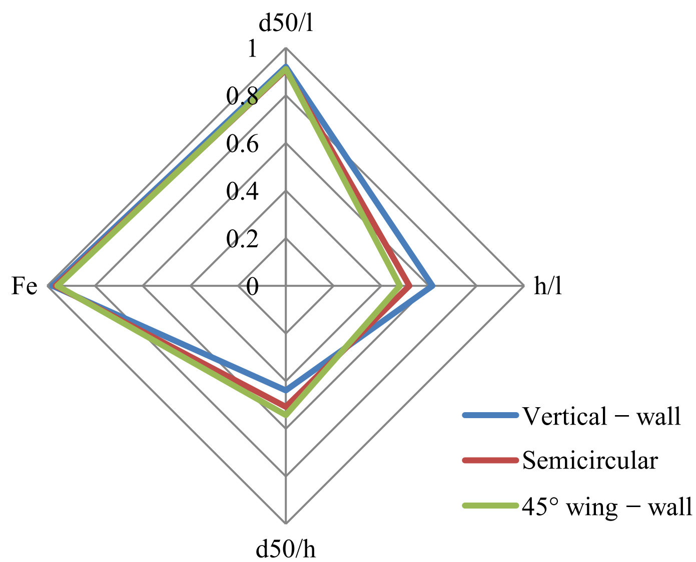

Fig 2. The relative importance of each input parameter using Pearson correlation coefficient

3.2. Assessing the best input combination

Although incorporating more input parameters in most of the cases can improve the performance of each algorithm in the training phase, including more parameters lead to more errors and to over-complicated algorithms (Fig 3a-c). For vertical-wall shape abutments, the best input combination is the No.3 (parameters F_e, d_{50}/l, h/l), as involving the additional parameter d_{50}/h

reduces the modeling prediction power and lead to more error. This result is in accordance with the outcomes of the correlation coefficient which showed that the d_{50}/h parameter has the lowest correlation with scour depth process.

For semicircular and 45° wing shape abutment, the input combination No.2 (F_e and d_{50}/l) has the highest effectiveness if compared to other input parameter combinations and results show that for semicircular shape abutment incorporating h/l and d_{50}/h lead to more degree of error. Although h/l is included on the empirical equations of Dey and Barbhuiya (2005) and Muzzammil (2010), our results show that this parameter is not crucially important in all cases and lead to more error in the modeling process.

Results show that the best input combinations have a 9.04%, 16.93% and 28.57% higher performance for vertical, semicircular and 45° wing abutment shape respectively, if compared to the worst input combination. This proves that determining the best input combination is significantly effective on the result and one of the most important steps in modeling process. Also, with the same input combination the result for different algorithms would be different, which reflects the different computation structures of the algorithms that each models developed is based on. Bonaldari et al. (2020) revealed that the best input combination for the Extreme Learning Machine (ELM) model is one in which all parameters (Fe, h/l, d_{50}/l, and Ks) are involved. Our results differ in this sense likely due to the different model structures and different computational capabilities.

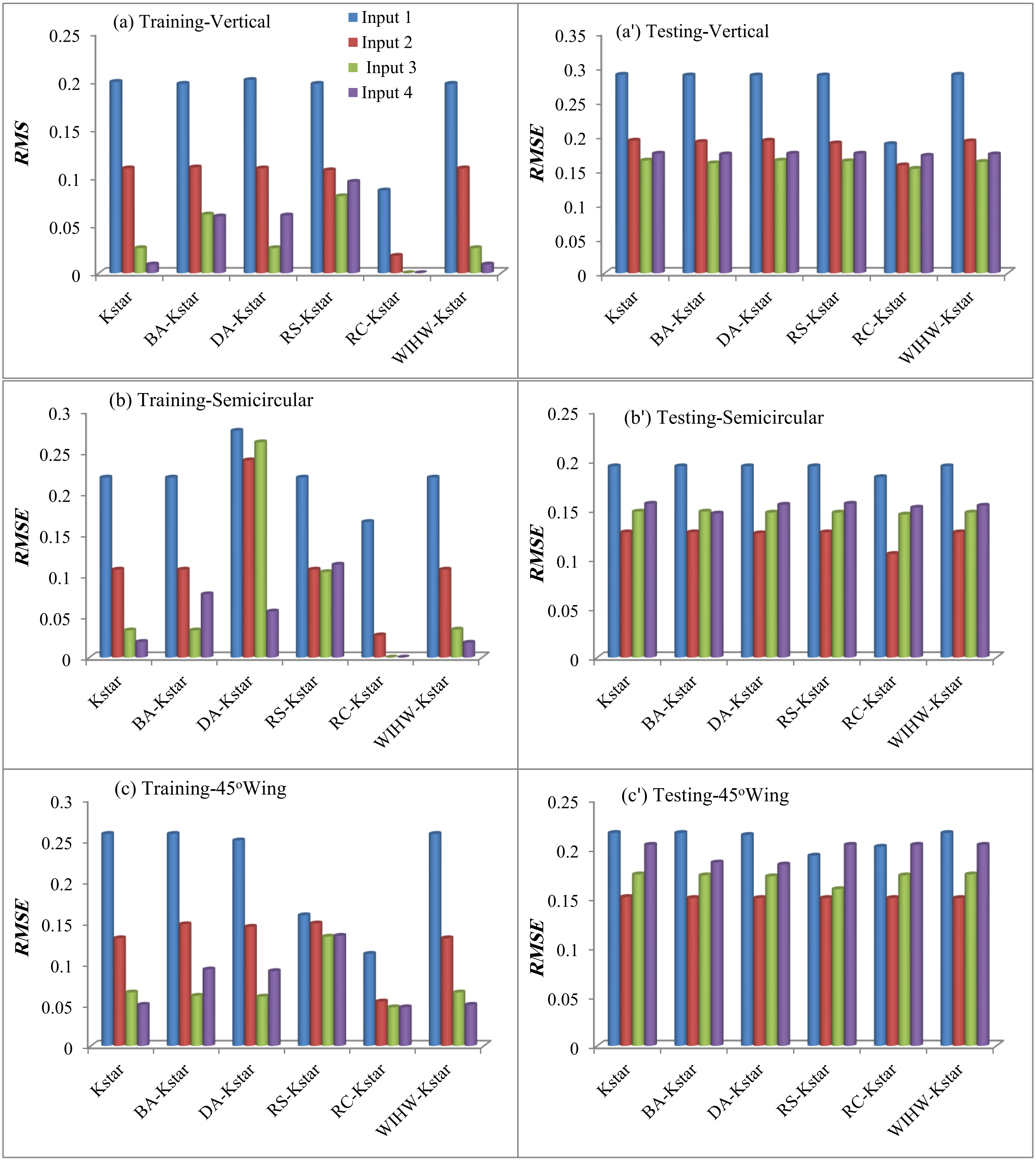

400 Fig 3. Use of quantitative metrics (RMSE) to determine the best input combination for the

models (the dataset is split in training and testing components).

3.3. Sensitivity analysis

A sensitivity analysis was carried out to determine the extent to which each parameter is effective on the results (Fig 4 and Table 4). According to the results, for vertical abutment shape, removing d_{50}/h, h/l, d_{50}/l and F_e implies a 5.74%, -3.44%, -16% and -18.4% change in the result (in terms of RMSE) revealing that F_e has the most significant effect on the results followed by d_{50}/l, d_{50}/h and h/l. Also, removing h/l, d_{50}/l and F_e increased RMSE while adding the d_{50}/h lead to a higher error. For semicircular shape abutment, removing d_{50}/h, h/l, d_{50}/l and F_e causes a 5.12%, 19.87%, -13.46% and -12.17% change in the results and shows that h/l is the most effective parameter on scour depth prediction for semicircular shape abutment followed by d_{50}/l, F_e and d_{50}/h. However, incorporating d_{50}/l and F_e and removing d_{50}/h, h/l lead to higher performances. Although removing h/l cause higher changes in the results, incorporating h/l and d_{50}/h leads to more error and reduces the models prediction power. For the 45° wing shape, removing d_{50}/h, h/l, d_{50}/l and F_e causes a 4.9%, 14.7%, -7.84% and -1.47% changes on the scour depth prediction. Indeed, h/l is the most important parameter followed by d_{50}/l, d_{50}/h and F_e, respectively. Also, similar to semicircular shape abutment, incorporating d_{50}/l and F_e and removing d_{50}/h, h/l leads to higher performances. This is in accordance with the outcomes of the r value and the determination of the most effective input parameter combination. Also, our result is in accordance with Bonakdari et al. (2020) which stated that the relative median sediment diameter (d_{50}/l) is the most effective parameter for the prediction of scour depth. Bonakdari et al. (2020) also stated that h/l is effective on the result and removing this parameter cause to about 1% higher error (which is overall not very significant). The opposite result can be obtained from different models structure and combining all dataset (rather than splitting them based on the abutment shape as in the present study). Our results are in accordance with the finding of Mohammadpour et al. (2013) that showed that incorporating h/l can lead to higher errors in the determination of the scour depths.

According to our results, the abutment geometry (i.e., l) has a significant effect on the scour occurrence process. As 45° and semicircular shape are more similar to each other if compared to the triangular shape, the effective parameters for 45° and semicircular shape are the same and different from those selected for the triangular shape.

Our results show that the approach flow depth (h) is not very effective on the overall scour depth, while flow velocity, transverse abutment length, and median sediment diameter are important. Azimi et al., (2019), Moradi et al., (2019) and Bonakdari et al., (2020) revealed that their best input combination was a combination of F_e, h/l, K_s, d_{50}/l. This definitely shows that the structure of the modeling approach has a crucial role on the selection of the input combination, which is resulting from different structure of each model. In our study, the best input combination for 45° wing wall and semicircular shapes involves F_e and d_{50}/l while for vertical wall the best combination includes F_e, d_{50}/l and h/l.

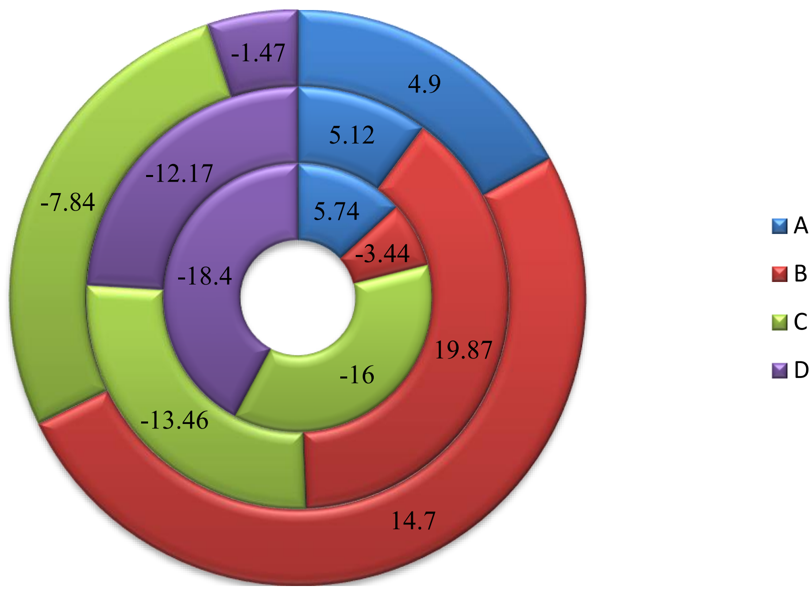

Fig 4. Percentage of changes applied for sensitivity analysis (the inner, middle and outer circles represent the vertical, semicircular, and 45° wing abutment shapes, respectively).

3.4. Evaluation of models performances

A visual comparison of the prediction power of the different machine learning models in terms of line graph and scatter plot is presented in Figure 5, 6 and 7 for vertical, semicircular and 45° wing, respectively. The figures present the values of scour depth obtained from the experimental data, and the values predicted by the stand-alone models of Kstar and its hybrid models of BA-Kstar, DA-Kstar, RC-Kstar, and WIHW-Kstar. Figure 6 also presents the results obtained using the empirical equations developed by Dey and Barbhuiya (2005) and Muzzammil (2010), and shows how all hybridized algorithm could enhance the performance of standalone Kstar algorithms while the empirical equations appear substantially overperformed.

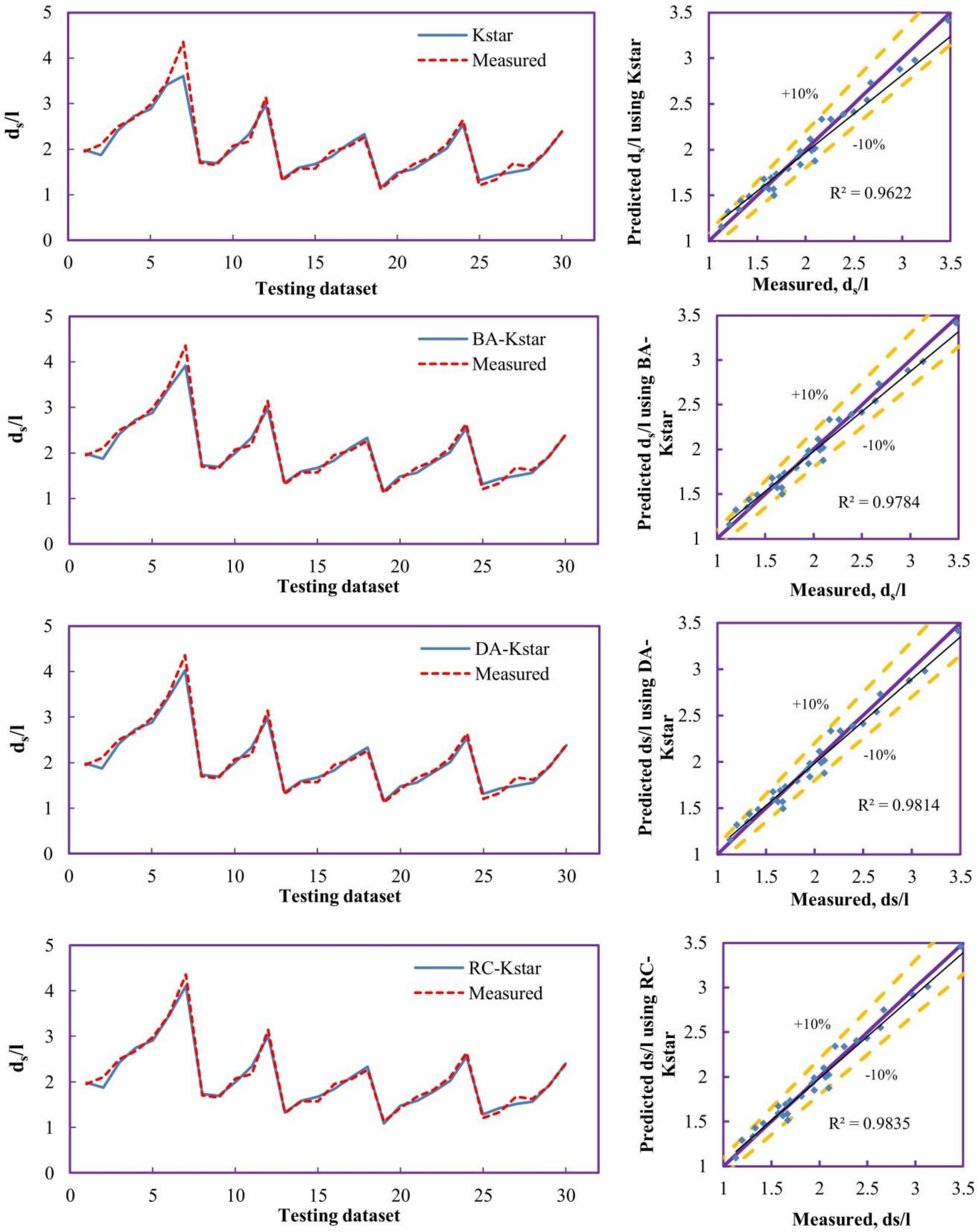

Kstar
Measured
d_s/l
Testing dataset
Predicted d_s/l using Kstar
Measured, d_s/l
+10%
-10%
$R^2 = 0.9622$
BA-Kstar
Measured
d_s/l
Testing dataset
Predicted d_s/l using BA-Kstar
Measured, d_s/l
+10%
-10%
$R^2 = 0.9784$
DA-Kstar
Measured
d_s/l
Testing dataset
Predicted ds/l using DA-Kstar
Measured, ds/l
+10%
-10%
$R^2 = 0.9814$
RC-Kstar
Measured
d_s/l
Testing dataset
Predicted ds/l using RC-Kstar
Measured, ds/l
+10%
-10%
$R^2 = 0.9835$

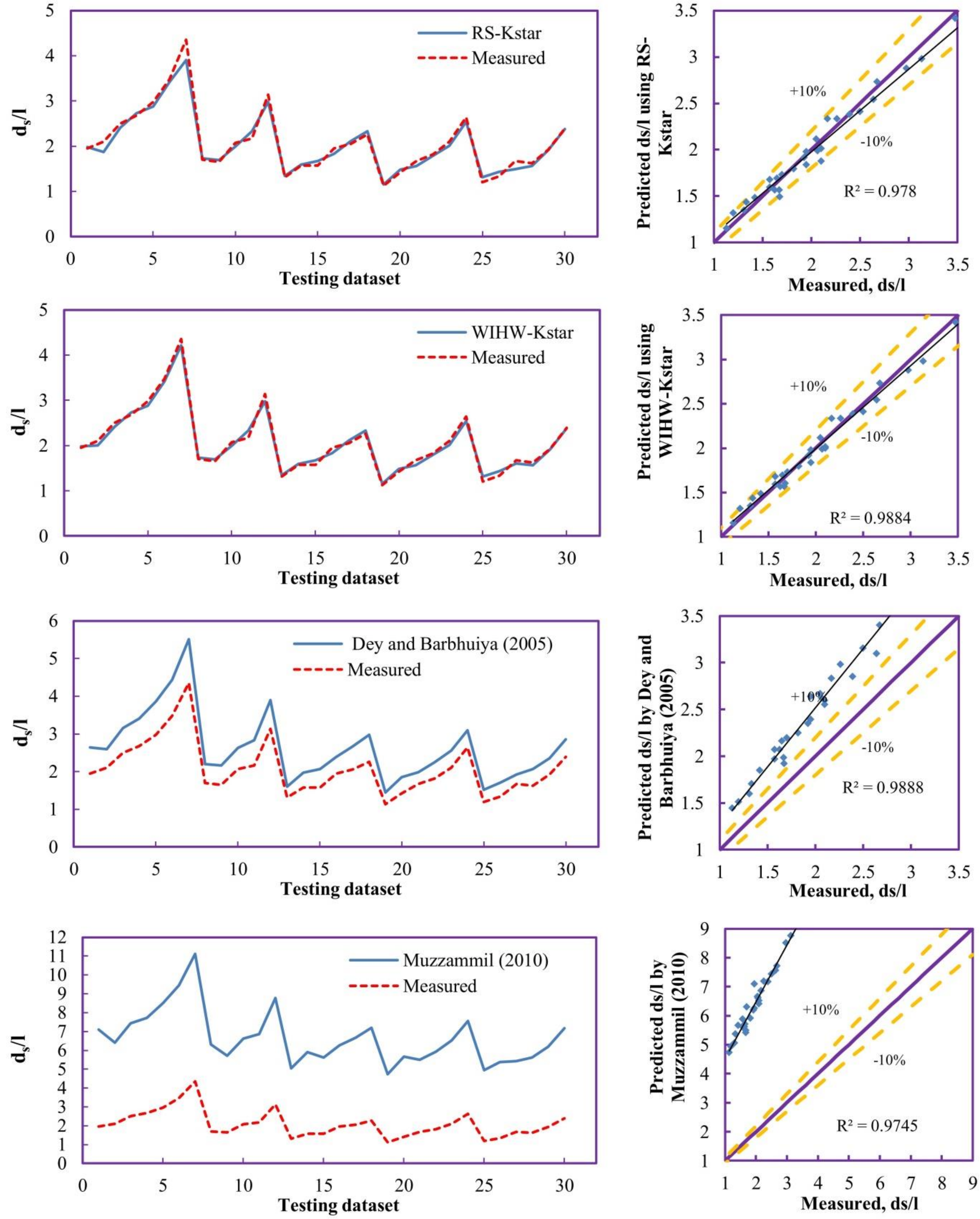

Fig 5. Line-graph and scatter plot of predicted vs. measured *ds/l* for vertical- wall shape abutment

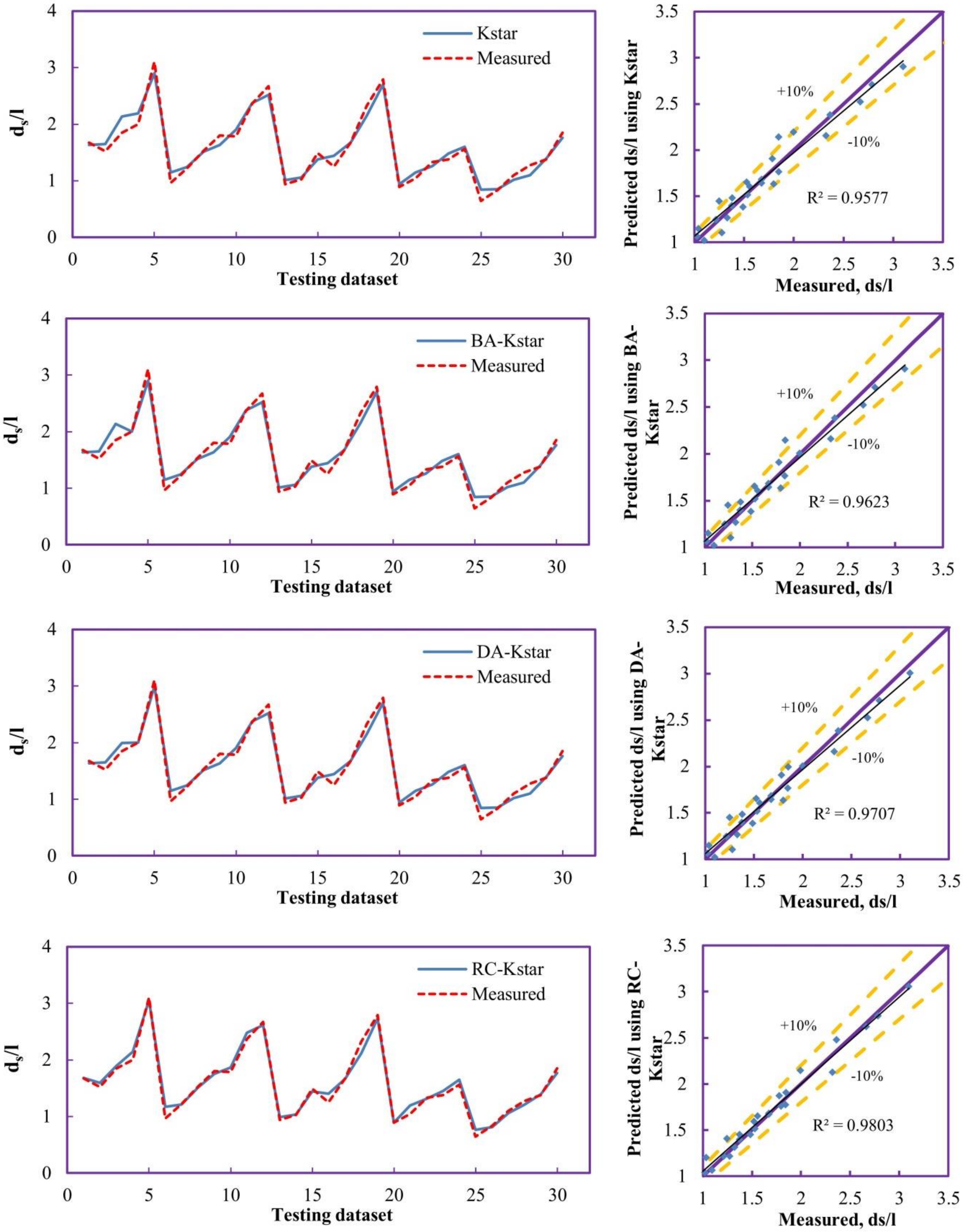
Kstar
Measured
ds/l
Testing dataset
Predicted ds/l using Kstar
Measured, ds/l
+10%
-10%
R² = 0.9577
BA-Kstar
Measured
Predicted ds/l using BA-Kstar
R² = 0.9623
DA-Kstar
Measured
Predicted ds/l using DA-Kstar
R² = 0.9707
RC-Kstar
Measured
Predicted ds/l using RC-Kstar
R² = 0.9803

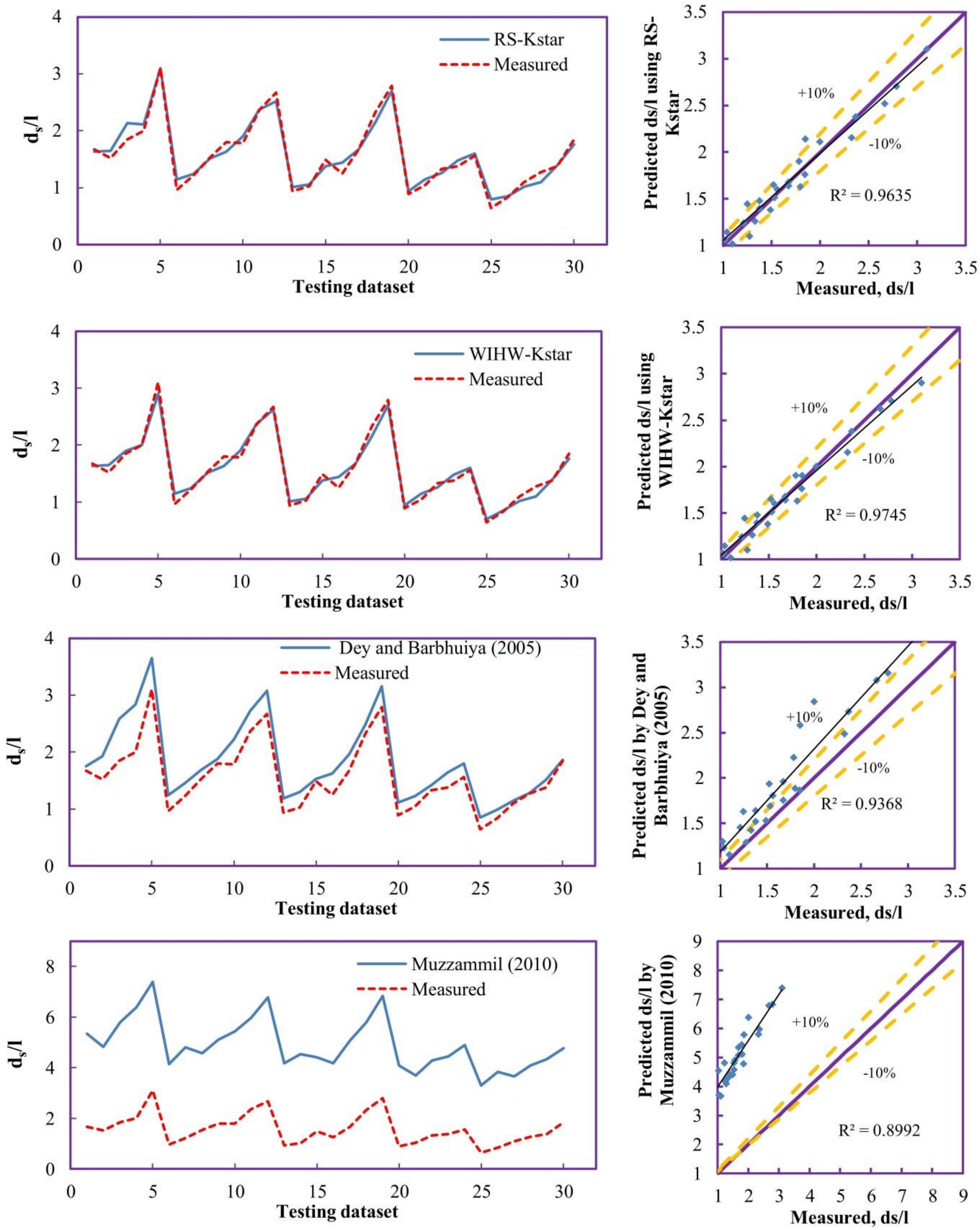

Fig 6. Line-graph and scatter plot of predicted vs. measured *ds/l* for semicircular shape abutment

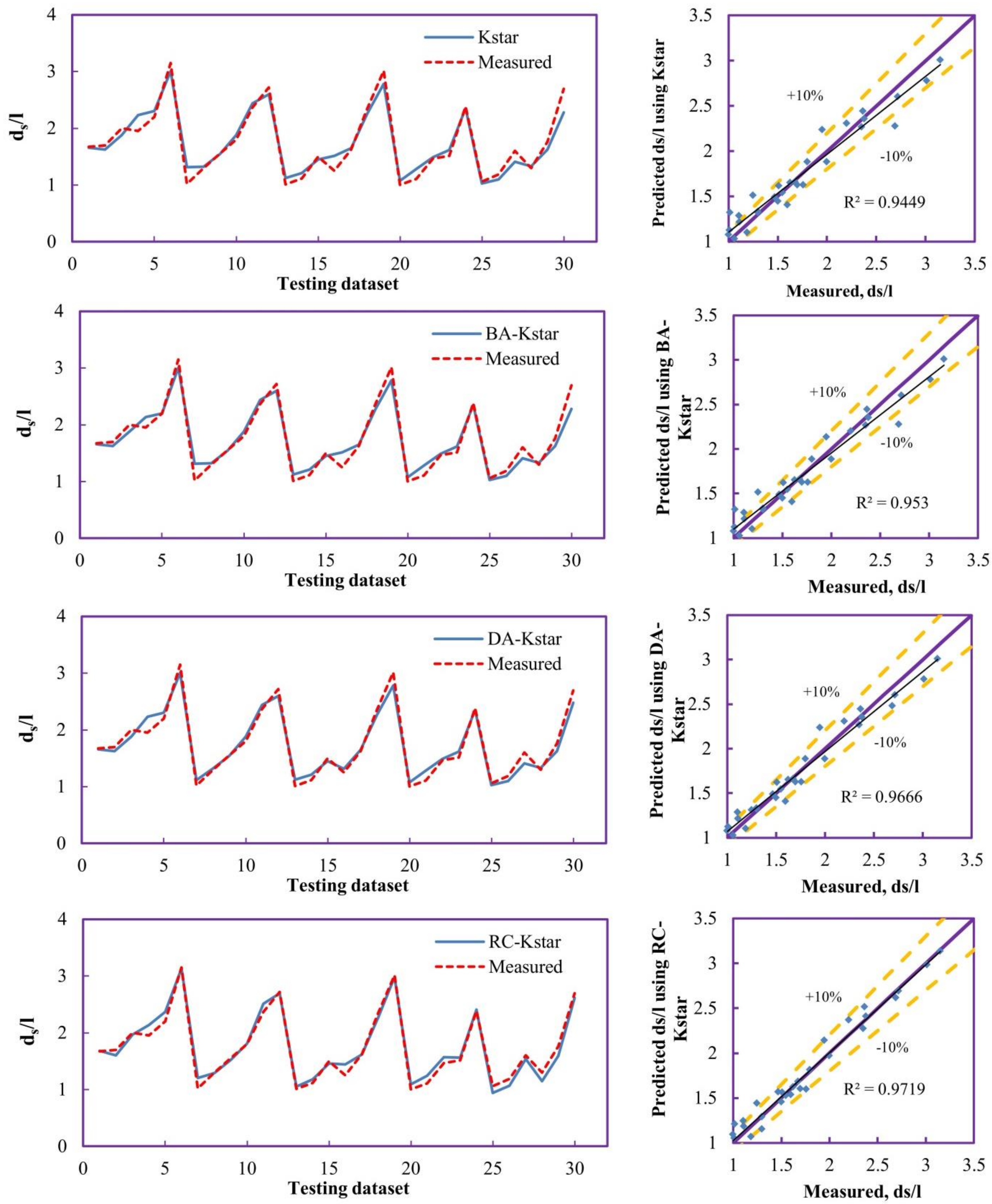

Kstar
Measured
d_s/l
Testing dataset
Predicted ds/l using Kstar
Measured, ds/l
+10%
-10%
$R^2 = 0.9449$
BA-Kstar
Measured
d_s/l
Testing dataset
Predicted ds/l using BA-Kstar
Measured, ds/l
+10%
-10%
$R^2 = 0.953$
DA-Kstar
Measured
d_s/l
Testing dataset
Predicted ds/l using DA-Kstar
Measured, ds/l
+10%
-10%
$R^2 = 0.9666$
RC-Kstar
Measured
d_s/l
Testing dataset
Predicted ds/l using RC-Kstar
Measured, ds/l
+10%
-10%
$R^2 = 0.9719$

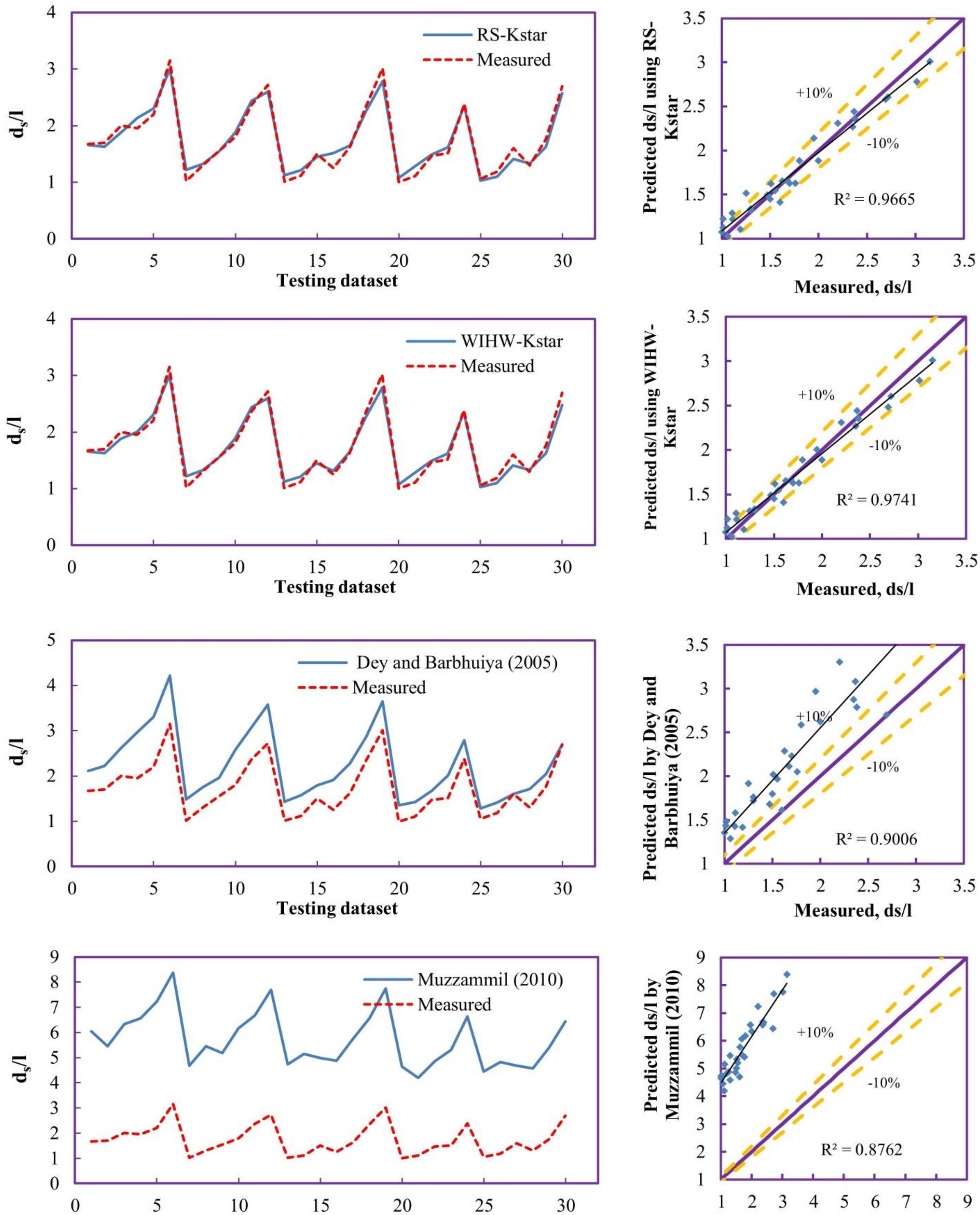

Fig 7. Line-graph and scatter plot of predicted vs. measured *ds/l* for 45° wing shape abutment

The violin plots of Figure 8 show that the WIHW-Kstar is able to predict the maximum ds/l values more accurately than other algorithms for vertical abutment. All developed algorithms are able to predict the first and third quartile and median relative scour depth values accurately while RC-Kstar predicted the minimum scour depth close to the measured values. Results also show that the equation proposed by Dey and Barbhuiya (2005) is more accurate than the equation proposed by Muzzammil (2010). Overall, the shape of violin plot of WIHW-Kstar is more similar to measured values compare to other models which have a similar distribution of data with measured dataset (Fig 8a). Although the violin plot generated by Dey and Barbhuiya (2005) equation have a similar shape of the measured values, their empirical equation fails to predict maximum, minimum, and median values with accuracy. Overall, the RC-Kstar model has a more similar shape of violin plot if compared with the measured values (Fig 8b). The RS-Kstar predicted better the maximum values while the WIHW-Kstar predicted better the minimum values. For 45° wing wall, all violin plot shapes of predicted dataset are far from the measured data. The RC-Kstar is able to predict the maximum values accurately while RS-Kstar and WIHW-Kstar are more accurate in predicting the minimum value of scour depth (Fig 8c). Also, none of the empirical equations are able to predict accurately the scour depth.

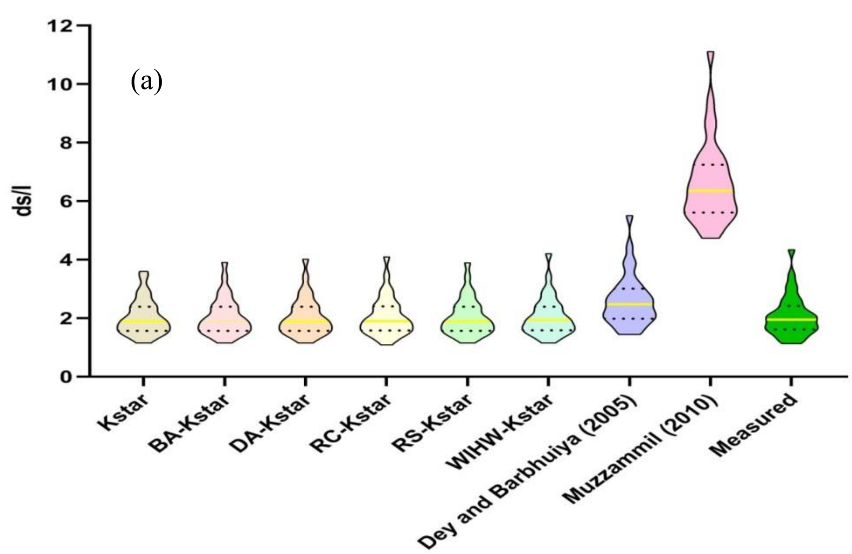

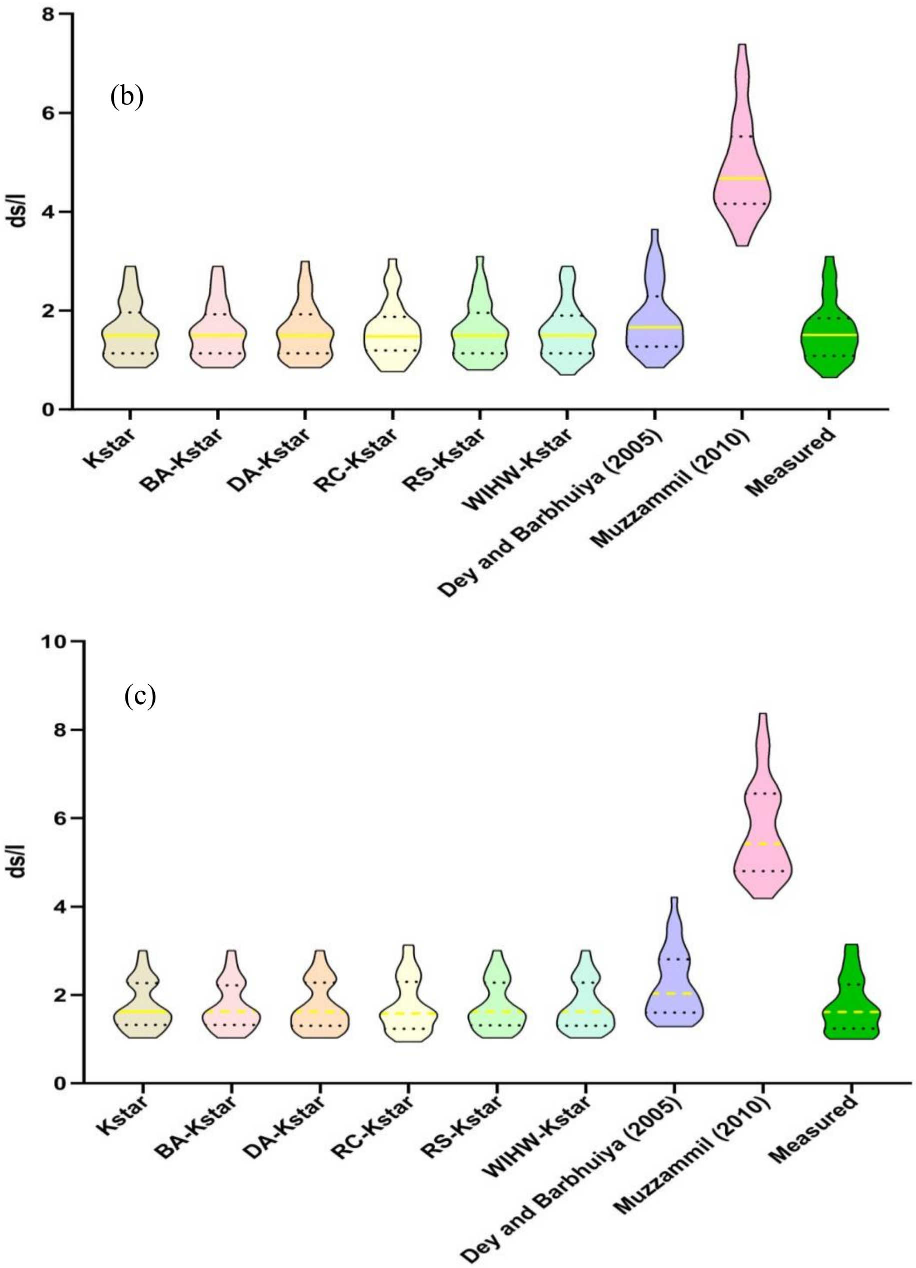

Fig 8. Violin plot of predicted Vs. measured scour depth prediction around (a) vertical, (b) semicircular and (c) 45° wing wall abutment.

The detailed results of the quantitative metrics for different abutment shape are showed on Table 5. The hybrid algorithm of WIWH-Kstar outperformed other algorithms in scour depth prediction for the vertical abutment shape (RMSE=0.084, RRMSE=4.081%, NSE=0.985, WI=0.996 and LM=0.857) followed by RC-Kstar (RMSE=0.097, RRMSE=4.711%, NSE=0.980, WI=0.994 and LM=0.850), RS-Kstar (RMSE=0.124, RRMSE=5.998%, NSE=0.968, WI=0.991 and LM=0.823), DA-Kstar (RMSE=0.111, RRMSE=5.363%, NSE=0.974, WI=0.993 and LM=0.830), BA-Kstar (RMSE=0.123, RRMSE=5.941%, NSE=0.968, WI=0.991 and LM=0.823), Kstar (RMSE=0.164, RRMSE=7.910%, NSE=0.944, WI=0.984 and LM=0.804), Dey and Barbhuiya (RMSE=0.522, RRMSE=25.125%, NSE=0.319, WI=0.883 and LM=-0.037) and Muzzammil (2010) (RMSE=4.618, RRMSE=222%, NSE=-42.375, WI=0.257 and LM=-7.764). Overall, all standalone and hybrid algorithms obtained excellent performance ($RRMSE \leq 10\%$), Dey and Barbhuiya (2005) had a fair performance ($20\% \leq RRMSE \leq 30\%$) while Muzzammil (2010) performed rather poorly (Despotovic et al, 2016). According to NSE, all standalone and hybrid algorithms had a very good performance (NSE>0.75) while Dey and Barbhuiya (2005) and Muzzammil (2010) performed rather poorly (Moriasi et al., 2007). Also, based on the RMSE metric BA, DA, RC, RS and WIHW could enhance the predictive power of the standalone algorithms of about 25%, 32.3%, 40.85%, 24.4% and 48.8% respectively. Finally, results based on the RMSE show that the WIHW-Kstar appears to be most effective model with about 8384% and 98.17% higher performance than Dey and Barbhuiya (2005) and Muzzammil (2010), respectively. According to our results, the RC-Kstar models outperforms all other algorithm for both semicircular and 45^{o} Wing abutment shape while Dey and Barbhuiya (2005) and Muzzammil (2010) had the lower performance. According to the RRMSE and NSE metrics, all standalone and hybrid algorithms had an excellent performance for both semicircular and 45^{o} Wing abutment.

It is interesting to note how BA, DA, RC, RS and WIHW could enhance the prediction power of the standalone algorithms of about 3.93%, 14.96%, 30.70%, 8.66% and 20.47% respectively for semicircular abutment (based on the RMSE metric). Also, the RC-Kstar is the most effective model and has about 72.92% and 97.37% higher performance than while Dey and Barbhuiya (2005) and Muzzammil (2010), respectively (based on the RMSE metric). According to the results of RMSE, BA, DA, RC, RS and WIHW could enhance the prediction power of the standalone algorithms of about 3.97%, 21.85%, 32.45%, 20.52% and 26.49%, respectively, for 45° wing abutment. Also, the result of the RC-Kstar is the most effective model, and has about 82.07% and 97.46% higher performance than while Dey and Barbhuiya (2005) and Muzzammil (2010), respectively.

Table 5. Quantitative performance of the tested models

Abutment shape	**Models**	**RMSE**	**RRMSE (%)**	**NSE**	**WI**	**LM**
Vertical	Kstar	0.164	7.91	0.944	0.984	0.804
	BA-Kstar	0.123	5.941	0.968	0.991	0.823
	DA-Kstar	0.111	5.363	0.974	0.993	0.830
	RC-Kstar	0.097	4.711	0.98	0.994	0.850
	RS-Kstar	0.124	5.998	0.968	0.991	0.823
	WIWH-Kstar	0.084	4.081	0.985	0.996	0.857
	Dey and Barbhuiya (2005)	0.522	25.125	0.319	0.883	-0.037
	Muzzammil (2010)	4.618	222	-42.375	0.257	-7.764
Semicircular	Kstar	0.127	8.069	0.954	0.987	0.775
	BA-Kstar	0.122	7.762	0.957	0.988	0.789
	DA-Kstar	0.108	6.913	0.966	0.99	0.806
	RC-Kstar	0.088	5.603	0.977	0.994	0.854
	RS-Kstar	0.116	7.365	0.961	0.989	0.799
	WIWH-Kstar	0.101	6.463	0.97	0.992	0.824
	Dey and Barbhuiya (2005)	0.325	20.668	0.698	0.938	0.435
	Muzzammil (2010)	3.355	213.036	-30.993	0.286	-6.145
45° Wing	Kstar	0.151	8.692	0.937	0.982	0.763
	BA-Kstar	0.145	8.319	0.942	0.983	0.777
	DA-Kstar	0.118	6.783	0.961	0.989	0.804
	RC-Kstar	0.102	5.853	0.971	0.992	0.833
	RS-Kstar	0.120	6.903	0.96	0.989	0.797
	WIWH-Kstar	0.111	6.38	0.966	0.99	0.813
	Dey and Barbhuiya (2005)	0.569	32.636	0.115	0.847	-0.01
	Muzzammil (2010)	4.012	229.88	-42.877	0.254	-7.018

The Kstar algorithm is able to match the observed values obtained in the flume experiments by Dey and Barbhuiya (2005) with higher performance than traditional empirical approaches and the other tested methods. Being based on heuristic search, the Kstar algorithm leads to considerable improvements in terms of both memory and runtime (Aljazzar and Leue, 2011). Because of the higher flexibility of the structures of the ensemble algorithms, in most of cases, these models show better performance than standalone algorithms (De'Ath and Fabricius, 2000).

Determining the proper combination of input parameters is one of the most important steps in developing a precise AI model. We investigated the combinations using a sensitivity analysis to find the most significant input variables to estimate the scour depth. F_e resulted one of the most important parameters in estimating scour depth for three shapes of abutments, probably because the flow velocity is embedded in the F_e parameter. Garde et al. (1961) noted that the optimum scour depth happens at the condition of threshold for the movement of sediments and that the flow rate defined in excess of Froude number has a major impact on the depth of the scour. In addition, Froehlich (1989) showed that the excess Froude influence the scour depth in a uniform sediment bed, under clear-water condition, and our results are in agreement with that. The other AI models proposed by Azimi et al. (2019), Bonakdari et al. (2020), Moradi et al. (2019) and Najafzadeh et al. (2013b) all mentioned that the influence of F_e parameter in the prediction of scour depth is remarkable.

By using the same dataset of Dey and Barbhuiya (2005) different researchers attempted to estimate scour depth by employing other AI appraoches (Azimi et al., 2019; Bonakdari et al., 2020; Moradi et al., 2019). Moradi et al. (2019) used a neuro-fuzzy-embedded subtractive clustering (ANFIS–SC) method to forecast scour depth and their results showed that ANFIS-SC with RMSE of 0.154 scored the better performance in estimating the scour depth. The application of ELM method in predicting scour depth was investigated by Bonakdari et al. (2020) that showed that the best ELM model can predict scour depth with RMSE of 0.177. In another research, Azimi et al., (2019) studied an application of a hybrid model as ANFIS-GA/SVD to predict scour depth and they concluded that their proposed model is robust in estimating scour depth with RMSE of 0.135. In our study we used a different ensemble-based models to the predict scour depth for each shape of abutments. For vertical-wall abutments the WIWH-Kstar model showed the best performance among all other models, with a RMSE of 0.084. In semicircular and 45° wing wall, the RC-Kstar (RMSE of 0.088 and 0.102, respectively) indicated higher accuracy in predicting scour depth. In comparison with other AI methods which were previously applied by different researchers, our proposed methods are more robust in scour depth estimations and have a higher prediction power. This is probably due to the fact that the model structure of our proposed algorithms work better than traditional models and it is better to model the data of each shape separately in order to avoid having to include in the analysis a shape factor.

The outcomes of the proposed models compared with the scour depth values which calculated from equations proposed by Dey and Barbhuiya (2005) and Muzzammil (2010) demonstrated that the proposed WIWH-Kstar and RC-Kstar for vertical wall, and semicircular and 45° wing wall respectively, predict more precisely the experimental scours than empirical approaches.

One of the main sources of uncertainty in our study refers to the extent of the dataset. Each set of data was about 100 raw data. In this sense, any further experimental dataset would allow to refine the modeling efforts. It is also worth pointing out that it would be recommendable to select dataset from several researchers to build a training dataset for algorithms. Also, a more extended dataset would allow a proper calibration and validation, and ideally a validation performed with data obtained in a different experimental setting.

5. Conclusion

Inaccurate predictions of scour depth (*ds*) at bridge abutment can cause the failure of strategic structures. Due to the complexity of the scour process with non-linearity structure, simple empirical equations are not able to predict ds accurately. In the present study, standalone Kstar model and five novel hybrid algorithm of bagging (BA), dagging (DA), random committee (RC), random subspace (RS), and weighted instance handler wrapper (WIHW) (i.e. BA-Kstar, DA-Kstar, RC-Kstar, RS-Kstar, WIWH-Kstar) were applied for *ds* prediction in a clear water (no sediment feeding) condition and the result were compared with two most common empirical equations as a benchmark. The results of the current study are the following:

- According to Pearson correlation coefficient, the F_e parameter has the highest effect on the scour depth prediction at each shape of Vertical – wall, Semicircular and 45° wing – wall, followed by d_{50}/l, h/l and d_{50}/h, respectively.
- For vertical-wall shape abutment, the best input is the combination of F_e, d_{50}/l, h/l parameters, and result shows that involving parameter of d_{50}/h reduces the modeling prediction power.
- For semicircular and 45° wing shape abutment, the input combination of F_e, d_{50}/l has the highest effectiveness.
- The sensitivity analysis revealed that F_e has the largest effect on the ds prediction around vertical abutment shape, while the h/l parameter has the great effect on the ds prediction around semicircular and 45° wing – wall abutment.

- The sensitivity analysis revealed that F_e, d_{50}/l and h/l increase the predictive power of the modeling for vertical abutment, while for semicircular and 45° wing – wall abutment incorporating d_{50}/l and F_e and removing d_{50}/h, and h/l cause to higher performance.
- Result showed that hybrid algorithm of WIHW-Kstar outperform of other algorithm for vertical abutment while RC-Kstar superior in ds prediction around semicircular and 45° wing abutment.
- According to NSE, all artificial intelligence models have a very good performance while the two empirical equations available in the literature have a much lower performance.
- BA, DA, RC, RS and WIHW could enhance prediction power of the standalone algorithms significantly.

Author Contributions: Conceptualization: KK and L.M; Modeling performance: KK; formal analysis: KK; Software: KK; writing—original draft preparation: KK, Z.S.K; Data collection: Z.S.K; review and editing: KK and L.M. All authors have read and agreed to the submitted version of the manuscript.

Conflicts of Interest: The authors declare no conflict of interest.

References

Abd El-Hady Rady, R., 2020. Prediction of local scour around bridge piers: artificial-intelligence-based modeling versus conventional regression methods. Appl. Water Sci. 10, 57. https://doi.org/10.1007/s13201-020-1140-4

Ahmad, M.W., Reynolds, J., Rezgui, Y., 2018. Predictive modelling for solar thermal energy systems: A comparison of support vector regression, random forest, extra trees and regression trees. J. Clean. Prod. 203, 810–821. https://doi.org/10.1016/j.jclepro.2018.08.207

Aljazzar, H., Leue, S., 2011. K*: A heuristic search algorithm for finding the k shortest paths. Artif. Intell. 175, 2129–2154. https://doi.org/10.1016/j.artint.2011.07.003

Amini, A., Melville, B.W., Ali, T.M., Ghazali, A.H., 2012. Clear-water local scour around pile groups in shallow-water flow. J. Hydraul. Eng. 138, 177–185. https://doi.org/10.1061/(ASCE)HY.1943-7900.0000488

Ataie-Ashtiani, B., Baratian-Ghorghi, Z., Beheshti, A.A., 2010. Experimental investigation of clear-water local scour of compound piers. J. Hydraul. Eng. 136, 343–351. https://doi.org/10.1061/(ASCE)0733-9429(2010)136:6(343)

Ataie-Ashtiani, B., Beheshti, A.A., 2006. Experimental investigation of clear-water local scour at pile groups. J. Hydraul. Eng. 132, 1100–1104. https://doi.org/10.1061/(ASCE)0733-9429(2006)132:10(1100)

Azamathulla, H.M., 2012. Gene-expression programming to predict scour at a bridge abutment. J. Hydroinformatics 14, 324–331. https://doi.org/10.2166/hydro.2011.135

Azamathulla, H.M., Ghani, A.A., Zakaria, N.A., 2009. ANFIS-based approach to predicting scour location of spillway. Proc. Inst. Civ. Eng. Water Manag. 162, 399–407. https://doi.org/10.1680/wama.2009.162.6.399

Azimi, H., Bonakdari, H., Ebtehaj, I., … S.T.-F.S. and, 2017, undefined, n.d. Evolutionary Pareto optimization of an ANFIS network for modeling scour at pile groups in clear water condition. Elsevier.

Azimi, H., Bonakdari, H., Ebtehaj, I., Shabanlou, S., Ashraf Talesh, S.H., Jamali, A., 2019. A pareto design of evolutionary hybrid optimization of ANFIS model in prediction abutment scour depth. Sadhana - Acad. Proc. Eng. Sci. 44. https://doi.org/10.1007/s12046-019-1153-6

Barbhuiya, A.K., 2003. Clear-water scour at abutments. Indian Institute of Technology, Kharagpur, India.

Bateni, S.M., Jeng, D.S., 2007. Estimation of pile group scour using adaptive neuro-fuzzy approach. Ocean Eng. 34, 1344–1354. https://doi.org/10.1016/j.oceaneng.2006.07.003

Bonakdari, H., Moradi, F., Ebtehaj, I., Gharabaghi, B., Sattar, A.A., Azimi, A.H., Radecki-Pawlik, A., 2020. A non-tuned machine learning technique for abutment scour depth in clear water condition. Water (Switzerland) 12, 301. https://doi.org/10.3390/w12010301

Breiman, L., 1996. Bagging predictors. Mach. Learn. 24, 123–140.

Bui, Duie Tien, Khosravi, K., Tiefenbacher, J., Nguyen, H., Kazakis, N., 2020. Improving prediction of water quality indices using novel hybrid machine-learning algorithms. Sci. Total Environ. 721. https://doi.org/10.1016/j.scitotenv.2020.137612

Cardoso, A.H., Bettess, R., 1999. Effects of time and channel geometry on scour at bridge abutments. J. Hydraul. Eng. 125, 388–398. https://doi.org/10.1061/(asce)0733-9429(1999)125:4(388)

Choubin, B., Darabi, H., Rahmati, O., Sajedi-Hosseini, F., Kløve, B., 2018. River suspended sediment modelling using the CART model: A comparative study of machine learning techniques. Sci. Total Environ. 615, 272–281. https://doi.org/10.1016/j.scitotenv.2017.09.293

Cleary, J.G., Trigg, L.E., 1995. K*: An Instance-based Learner Using an Entropic Distance Measure, in: Machine Learning Proceedings 1995. pp. 108–114. https://doi.org/10.1016/b978-1-55860-377-6.50022-0

Coleman, S.E., Lauchlan, C.S., Melville, B.W., 2003. Développement de l'affouillement en eau claire aux butées de pont. J. Hydraul. Res. 41, 521–531. https://doi.org/10.1080/00221680309499997

De'Ath, G., Fabricius, K.E., 2000. Classification and regression trees: A powerful yet simple technique for ecological data analysis. Ecology 81, 3178–3192. https://doi.org/10.1890/0012-

9658(2000)081[3178:CARTAP]2.0.CO;2

Dey, S., 1997. Local Scour at Piers, part I: A Review of Development of Research. Int. J. Sediment Res. 12, 23–44.

Dey, S., Barbhuiya, A.K., 2005. Time Variation of Scour at Abutments. J. Hydraul. Eng. 131, 11–23. https://doi.org/10.1061/(ASCE)0733-9429(2005)131:1(11)

Dey, S., Barbhuiya, A.K., 2004. Clear-water scour at abutments in thinly armored beds. J. Hydraul. Eng. 130, 622–634. https://doi.org/10.1061/(ASCE)0733-9429(2004)130:7(622)

Dey, S., Lambert, M.F., 2005. Reynolds Stress and Bed Shear in Nonuniform Unsteady Open-Channel Flow. J. Hydraul. Eng. 131, 610–614. https://doi.org/10.1061/(ASCE)0733-9429(2005)131:7(610)

Dietterich, T.G., 2000. An experimental comparison of three methods for constructing ensembles of decision trees: bagging, boosting, and randomization. Mach. Learn. 40, 139–157. https://doi.org/10.1023/A:1007607513941

Ebtehaj, I., Bonakdari, H., Moradi, F., Gharabaghi, B., Khozani, Z.S., Sheikh Khozani, Z., 2018. An integrated framework of Extreme Learning Machines for predicting scour at pile groups in clear water condition. Coast. Eng. 135, 1–15. https://doi.org/10.1016/j.coastaleng.2017.12.012

Firat, M., Gungor, M., 2009. Generalized Regression Neural Networks and Feed Forward Neural Networks for prediction of scour depth around bridge piers. Adv. Eng. Softw. 40, 731–737. https://doi.org/10.1016/j.advengsoft.2008.12.001

Froehlich, D.C., 1989. Local scour at bridge abutments, in: Proceedings of the National Conference on Hydraulic Engineering. New Orleans, USA, pp. 13–18.

Garde, R.J., Subramanya, K.S. Nambudripad, K.D., 1961. Study of scour around spur-dikes. J. Hydraul. Div. 87, 23–37.

Gazi, A.H., Afzal, M.S., Dey, S., 2019. Scour around piers underwaves: Current status of research and its future prospect. Water (Switzerland). https://doi.org/10.3390/w11112212

Guven, A., Azamathulla, H.M., 2012. A comparative study of predicting scour around a circular pile. ICE Marit. Eng. 165, 31–40.

Guven, A., Gunal, M., 2008. Genetic programming approach for prediction of local scour downstream of hydraulic structures. J. Irrig. Drain. Eng. 134, 241–249. https://doi.org/10.1061/(ASCE)0733-9437(2008)134:2(241)

Hamidi, A., Siadatmousavi, S.M., 2018. Numerical simulation of scour and flow field for different arrangements of two piers using SSIIM model. Ain Shams Eng. J. 9, 2415–2426. https://doi.org/10.1016/j.asej.2017.03.012

Harikumar V, S.T.,, M., Kumar, A., K, A.P., Michael, P., P, A.P., E, N., 2018. Modelling of Scour Depth Around Bridge Piers using Artificial Neural Network (ANN), International Journal of Engineering Research & Technology. IJERT-International Journal of Engineering Research & Technology.

Ho, T.K., 1998. The random subspace method for constructing decision forests. IEEE Trans. Pattern Anal. Mach. Intell. 20, 832–844. https://doi.org/10.1109/34.709601

Hooshyaripor, F., Tahershamsi, A., 2013. Comparing the Performance of Neural Networks for Predicting

Peak Outflow from Breached Embankments when Back Propagation Algorithms Meet Evolutionary Algorithms. Int. J. Hydraul. Eng. 1, 55–67. https://doi.org/10.5923/j.ijhe.20120106.01

Hooshyaripor, F., Tahershamsi, A., Golian, S., 2014. Application of copula method and neural networks for predicting peak outflow from breached embankments. J. Hydro-Environment Res. 8, 292–303. https://doi.org/10.1016/j.jher.2013.11.004

Hosseini, K., Karami, H., Hosseinjanzadeh, H., Ardeshir, A., 2016. Prediction of time-varying maximum scour depth around short abutments using soft computing methodologies - A comparative study. KSCE J. Civ. Eng. 20, 2070–2081. https://doi.org/10.1007/s12205-015-0115-8

Jahangirzadeh, A., Basser, H., Akib, S., Karami, H., Naji, S., Shamshirband, S., 2014. Experimental and numerical investigation of the effect of different shapes of collars on the reduction of scour around a single bridge pier. PLoS One 9, e98592. https://doi.org/10.1371/journal.pone.0098592

Kandasamy, I.K., 1989. Aubtment scour. Auckland,New Zealand.

Kaya, A., 2010. Artificial neural network study of observed pattern of scour depth around bridge piers. Comput. Geotech. 37, 413–418. https://doi.org/10.1016/j.compgeo.2009.10.003

Khosravi, K., Mao, L., Kisi, O., Yaseen, Z.M., Shahid, S., 2018. Quantifying hourly suspended sediment load using data mining models: Case study of a glacierized Andean catchment in Chile. J. Hydrol. 567, 165–179. https://doi.org/10.1016/j.jhydrol.2018.10.015

Khosronejad, A., Diplas, P., Angelidis, D., Zhang, Z., Heydari, N., Sotiropoulos, F., 2020. Scour depth prediction at the base of longitudinal walls: a combined experimental, numerical, and field study. Environ. Fluid Mech. 20, 459–478. https://doi.org/10.1007/s10652-019-09704-x

Kim, H.S., Nabi, M., Kimura, I., Shimizu, Y., 2014. Numerical investigation of local scour at two adjacent cylinders. Adv. Water Resour. 70, 131–147. https://doi.org/10.1016/j.advwatres.2014.04.018

Kothyari, U.C., Garde, R.C.J., Ranga Raju, K.G., 1992. Temporal Variation of Scour Around Circular Bridge Piers. J. Hydraul. Eng. 118, 1091–1106. https://doi.org/10.1061/(ASCE)0733-9429(1992)118:8(1091)

Kotsiantis, S., 2011. Combining bagging, boosting, rotation forest and random subspace methods. Artif. Intell. Rev. 35, 223–240. https://doi.org/10.1007/s10462-010-9192-8

Kwan, T., 1988. A study of abutment scour. Auckland.

Melville, B.W., Raudkivi, A.J., 1977. Caracteristiques de l'ecoulement dans des conditions d'affouillement localisees au voisinage immediat des piles d'un pont. J. Hydraul. Res. 15, 373–380. https://doi.org/10.1080/00221687709499641

Melville, B.W., Sutherland, A.J., 1988. Design method for local scour at bridge piers. J. Hydraul. Eng. 114, 1210–1226. https://doi.org/10.1061/(ASCE)0733-9429(1988)114:10(1210)

Mohammadpour, R., Ghani, A.A., Azamathulla, H.M., 2013. Estimation of dimension and time variation of local scour at short abutment. Int. J. River Basin Manag. https://doi.org/10.1080/15715124.2013.772522

Moonen, P., Allegrini, J., 2015. Employing statistical model emulation as a surrogate for CFD. Environ. Model. Softw. 72, 77–91. https://doi.org/10.1016/j.envsoft.2015.06.007

Moradi, F., Bonakdari, H., Kisi, O., Ebtehaj, I., Shiri, J., Gharabaghi, B., 2019. Abutment scour depth modeling using neuro-fuzzy-embedded techniques. Mar. Georesources Geotechnol. 37, 190–200. https://doi.org/10.1080/1064119X.2017.1420113

Moriasi, D.N., Arnold, J.G.J.G.J.G., Van Liew, M.W.M.W.M.W., Bingner, R.L., Harmel, R.D.D., Veith, T.L.T.L.T.L.T.L., Binger, R.L., Harmel, R.D.D., Veith, T.L.T.L.T.L.T.L., Bingner, R.L., Harmel, R.D.D., Veith, T.L.T.L.T.L.T.L., 2007. Model evaluation guidelines for systematic quantification of accuracy in watershed simulations. Trans. ASABE 50, 885–900. https://doi.org/10.13031/2013.23153

Muzzammil, M., 2010. ANFIS approach to the scour depth prediction at a bridge abutment. J. Hydroinformatics 12, 474–485. https://doi.org/10.2166/hydro.2010.004

Muzzammil, M., 2008. Application of neural networks to scour depth prediction at the bridge abutments. Eng. Appl. Comput. Fluid Mech. 2, 30–40. https://doi.org/10.1080/19942060.2008.11015209

Najafzadeh, M., Balf, M.R., Rashedi, E., 2016. Prediction of maximum scour depth around piers with debris accumulation using EPR, MT, and GEP models. J. Hydroinformatics 18, 867–884. https://doi.org/10.2166/hydro.2016.212

Najafzadeh, M., Barani, G.A., Hessami Kermani, M.R., 2013a. GMDH based back propagation algorithm to predict abutment scour in cohesive soils. Ocean Eng. 59, 100–106. https://doi.org/10.1016/j.oceaneng.2012.12.006

Najafzadeh, M., Barani, G.A., Kermani, M.R.H., 2013b. Abutment scour in clear-water and live-bed conditions by GMDH network. Water Sci. Technol. 67, 1121–1128. https://doi.org/10.2166/wst.2013.670

Najafzadeh, M., Lim, S.Y., 2015. Application of improved neuro-fuzzy GMDH to predict scour depth at sluice gates. Earth Sci. Informatics 8, 187–196. https://doi.org/10.1007/s12145-014-0144-8

Namaee, M.R., Sui, J., 2019. Impact of armour layer on the depth of scour hole around side-by-side bridge piers under ice-covered flow condition. J. Hydrol. Hydromechanics 67, 240–251. https://doi.org/10.2478/johh-2019-0010

Nourani, V., Komasi, M., Alami, M.T., 2012. Hybrid Wavelet-Genetic Programming Approach to Optimize ANN Modeling of Rainfall-Runoff Process. J. Hydrol. Eng. 17, 724–741. https://doi.org/10.1061/(ASCE)HE.1943-5584.0000506

Oliveto, G., Hager, W.H., 2002. Temporal evolution of clear-water pier and abutment scour. J. Hydraul. Eng. 128, 811–820. https://doi.org/10.1061/(ASCE)0733-9429(2002)128:9(811)

Omara, H., Elsayed, S.M., Abdeelaal, G.M., Abd-Elhamid, H.F., Tawfik, A., 2019. Hydromorphological Numerical Model of the Local Scour Process Around Bridge Piers. Arab. J. Sci. Eng. 44, 4183–4199. https://doi.org/10.1007/s13369-018-3359-z

Oza, N.C., 2005. Online bagging and boosting, in: Conference Proceedings - IEEE International Conference on Systems, Man and Cybernetics. pp. 2340–2345. https://doi.org/10.1109/icsmc.2005.1571498

Parsaie, A., Haghiabi, A.H., Moradinejad, A., 2019. Prediction of Scour Depth below River Pipeline using Support Vector Machine. KSCE J. Civ. Eng. 23, 2503–2513. https://doi.org/10.1007/s12205-019-1327-0

Raudkivi, A.J., Ettema, R., 1983. Clear-water scour at cylindrical piers. J. Hydraul. Eng. 109, 338–350. https://doi.org/10.1061/(ASCE)0733-9429(1983)109:3(338)

Sheikh Khozani, Z., Khosravi, K., Pham, B.T., Kløve, B., Wan Mohtar, W.H.M., Yaseen, Z.M., 2019. Determination of compound channel apparent shear stress: application of novel data mining models. J. Hydroinformatics 21, 798–811. https://doi.org/10.2166/hydro.2019.037

Sheppard, D.M., Odeh, M., Glasser, T., 2004. Large scale clear-water local pier scour experiments. J. Hydraul. Eng. 130, 957–963. https://doi.org/10.1061/(ASCE)0733-9429(2004)130:10(957)

Sihag, P., Singh, B., Sepah Vand, A., Mehdipour, V., 2020. Modeling the infiltration process with soft computing techniques. ISH J. Hydraul. Eng. 26, 138–152. https://doi.org/10.1080/09715010.2018.1464408

Singh, R.K., Pandey, M., Pu, J.H., Pasupuleti, S., Villuri, V.G.K., 2020. Experimental study of clear-water contraction scour. Water Supply 20, 943–952. https://doi.org/10.2166/ws.2020.014

Sun, S., Zhang, C., 2007. The selective random subspace predictor for traffic flow forecasting. IEEE Trans. Intell. Transp. Syst. 8, 367–373. https://doi.org/10.1109/TITS.2006.888603

Ting, K.M., Witten, I.H., 1997. Stacking bagged and dagged models. Proc. of ICML'97 367–375.

Török, G.T., Baranya, S., Rüther, N., Spiller, S., 2014. Laboratory analysis of armor layer development in a local scour around a groin, in: Proceedings of the International Conference on Fluvial Hydraulics, RIVER FLOW 2014. pp. 1455–1462. https://doi.org/10.1201/b17133-194

Wong, W., 1982. Scour at bridge abutments. New Zealand.

Yan, T., Chen, L., Xu, M., Zhou, M., 2012. Siphon pipeline resistance characteristic research, in: Procedia Engineering. pp. 99–104. https://doi.org/10.1016/j.proeng.2012.01.689

Yang, F., Liu, S.H., Wu, Y.L., Tang, X.L., 2005. Lattice Boltzmann subgrid model for lid-driven cavity flow. J. Hydrodyn. 17, 289–294. https://doi.org/10.1115/HT-FED2004-56100

Yang, Y., Melville, B.W., Macky, G.H., Shamseldin, A.Y., 2020. Experimental study on local scour at complex bridge pier under combined waves and current. Coast. Eng. 160, 103730. https://doi.org/10.1016/j.coastaleng.2020.103730

Yaseen, Z.M., Ebtehaj, I., Bonakdari, H., Deo, R.C., Danandeh Mehr, A., Mohtar, W.H.M.W., Diop, L., El-shafie, A., Singh, V.P., 2017. Novel approach for streamflow forecasting using a hybrid ANFIS-FFA model. J. Hydrol. 554, 263–276. https://doi.org/10.1016/j.jhydrol.2017.09.007

Yazdandoost, F., Birgani, Y.T., 2011. Bridge pier scour depth prediction using Artificial Neural Networks, in: The 7th IAHR Symposium on River, Coastal and Estuarine Morphodynamics. Beijing, China.